

Table 3. Relationship between liver-intestine cadherin (LI-cadherin) or epidermal growth factor receptor (EGFR) and clinicopathologic characteristics of gastric cancer

	LI-cadherin			EGFR		
	Positive (%)	Negative	P-value†	Positive (%)	Negative	P-value†
T grade						
T1	10 (23)	33	0.0254	0 (0)	43	<0.0001
T2/3/4	48 (44)	51		33 (30)	76	
N grade						
N0	17 (27)	46	0.0186	6 (10)	57	0.0025
N1/2/3	41 (46)	48		27 (30)	62	
Stage						
I/II	25 (31)	55	0.0689	10 (13)	70	0.0054
III/IV	33 (46)	39		23 (32)	49	
Histology						
Intestinal	33 (43)	43	0.2424	11 (14)	65	0.0481
Diffuse	25 (33)	51		22 (29)	54	

†Fisher's exact test.

observations indicate that the EGFR signaling pathway plays an important role in regulating intestinal epithelial cell production. In the light of these previous studies and ours, it is suspected that EGFR drives GC development through wide-ranging signaling pathways, and also induces intestinal phenotypes in GC by stimulation of LI-cadherin expression.

In summary, this study yielded a list of genes that were upregulated by EGFR activation in GC. We found that LI-cadherin is induced by EGFR, and overexpression of LI-cadherin is associated with the intestinal mucin phenotype. These results suggest that, in addition to CDX2, EGFR activation is involved in LI-cadherin expression in GC, and that EGFR may induce intestinal differentiation through upregulating LI-cadherin expression in a CDX2-independent manner.

Acknowledgments

We thank Mr Shinichi Norimura for his excellent technical assistance and advice. This work was carried out with the kind cooperation of the Research Center for Molecular Medicine, Faculty of Medicine, Hiroshima University (Hiroshima, Japan). We thank the Analysis Center of Life Science, Hiroshima University, for the use of their facilities. This work was supported in part by Grants-in-Aid for Cancer Research from

the Ministry of Education, Culture, Science, Sports, and Technology of Japan, in part by a Grant-in-Aid for the Third Comprehensive 10-Year Strategy for Cancer Control and for Cancer Research from the Ministry of Health, Labor and Welfare of Japan, and in part by a grant (07-23911) from the Princess Takamatsu Cancer Research Fund.

Disclosure Statement

The authors have no conflict of interest.

Abbreviations

CDH17	cadherin 17
CDX2	caudal type homeobox 2
EGF	epidermal growth factor
EGFR	epidermal growth factor receptor
G type	gastric type
GC	gastric cancer
GI type	gastric and intestinal mixed type
I type	intestinal type
LI-cadherin	liver-intestine cadherin
N type	unclassified type
TGF- α	transforming growth factor- α

References

- Crew KD, Neugut AI. Epidemiology of gastric cancer. *World J Gastroenterol* 2006; **12**: 354–62.
- Yasui W, Sentani K, Sakamoto N, Anami K, Naito Y, Oue N. Molecular pathology of gastric cancer: research and practice. *Pathol Res Pract* 2011; **207**: 608–12.
- Kang MJ, Ryu BK, Lee MG *et al*. NF-kappaB activates transcription of the RNA-binding factor HuR, via PI3K-AKT signaling, to promote gastric tumorigenesis. *Gastroenterology* 2008; **135**: 2030–42.
- Regalo G, Resende C, Wen X *et al*. C/EBP alpha expression is associated with homeostasis of the gastric epithelium and with gastric carcinogenesis. *Lab Invest* 2010; **90**: 1132–9.
- Yu HG, Ai YW, Yu LL *et al*. Phosphoinositide 3-kinase/Akt pathway plays an important role in chemoresistance of gastric cancer cells against etoposide and doxorubicin induced cell death. *Int J Cancer* 2008; **122**: 433–43.
- Yamamoto H, Kitadai Y, Yamamoto H *et al*. Laminin gamma2 mediates Wnt5a-induced invasion of gastric cancer cells. *Gastroenterology* 2009; **137**: 242–52.
- Mitani Y, Oue N, Matsumura S *et al*. Reg IV is a serum biomarker for gastric cancer patients and predicts response to 5-fluorouracil-based chemotherapy. *Oncogene* 2007; **26**: 4383–93.
- Tahara E, Sumiyoshi H, Hata J *et al*. Human epidermal growth factor in gastric carcinoma as a biologic marker of high malignancy. *Jpn J Cancer Res* 1986; **77**: 145–52.
- Yasui W, Hata J, Yokozaki H *et al*. Interaction between epidermal growth factor and its receptor in progression of human gastric carcinoma. *Int J Cancer* 1988; **41**: 211–17.
- Yasui W, Sumiyoshi H, Hata J *et al*. Expression of epidermal growth factor receptor in human gastric and colonic carcinomas. *Cancer Res* 1988; **48**: 137–41.
- Ito R, Kitadai Y, Kyo E *et al*. Interleukin 1 alpha acts as an autocrine growth stimulator for human gastric carcinoma cells. *Cancer Res* 1993; **53**: 4102–6.
- Yoshida K, Tsujino T, Yasui W *et al*. Induction of growth factor-receptor and metalloproteinase genes by epidermal growth factor and/or transforming growth factor-alpha in human gastric carcinoma cell line MKN-28. *Jpn J Cancer Res* 1990; **81**: 793–8.
- Berndorff D, Gessner R, Kreft B *et al*. Liver-intestine cadherin: molecular cloning and characterization of a novel Ca(2+)-dependent cell adhesion molecule expressed in liver and intestine. *J Cell Biol* 1994; **125**: 1353–69.
- Sheng G, Bernabe KQ, Guo J, Warner BW. Epidermal growth factor receptor-mediated proliferation of enterocytes requires p21waf1/cip1 expression. *Gastroenterology* 2006; **131**: 153–64.

- 15 Motoshita J, Nakayama H, Taniyama K, Matsusaki K, Yasui W. Molecular characteristics of differentiated-type gastric carcinoma with distinct mucin phenotype: LI-cadherin is associated with intestinal phenotype. *Pathol Int* 2006; **56**: 200–5.
- 16 Hinoi T, Lucas PC, Kuick R, Hanash S, Cho KR, Fearon ER. CDX2 regulates liver intestine-cadherin expression in normal and malignant colon epithelium and intestinal metaplasia. *Gastroenterology* 2002; **123**: 1565–77.
- 17 Nagao K, Togawa N, Fujii K *et al.* Detecting tissue-specific alternative splicing and disease-associated aberrant splicing of the PTCH gene with exon junction microarrays. *Hum Mol Genet* 2005; **14**: 3379–88.
- 18 Oue N, Hamai Y, Mitani Y *et al.* Gene expression profile of gastric carcinoma: identification of genes and tags potentially involved in invasion, metastasis, and carcinogenesis by serial analysis of gene expression. *Cancer Res* 2004; **64**: 2397–405.
- 19 Hasegawa S, Furukawa Y, Li M *et al.* Genome-wide analysis of gene expression in intestinal-type gastric cancers using a complementary DNA microarray representing 23,040 genes. *Cancer Res* 2002; **62**: 7012–17.
- 20 Inoue H, Matsuyama A, Mimori K, Ueo H, Mori M. Prognostic score of gastric cancer determined by cDNA microarray. *Clin Cancer Res* 2002; **8**: 3475–9.
- 21 Zembutsu H, Ohnishi Y, Tsunoda T *et al.* Genome-wide cDNA microarray screening to correlate gene expression profiles with sensitivity of 85 human cancer xenografts to anticancer drugs. *Cancer Res* 2002; **62**: 518–27.
- 22 Oue N, Sentani K, Sakamoto N *et al.* Characteristic gene expression in stromal cells of gastric cancers among atomic-bomb survivors. *Int J Cancer* 2009; **124**: 1112–21.
- 23 Kondo T, Oue N, Yoshida K *et al.* Expression of POT1 is associated with tumor stage and telomere length in gastric carcinoma. *Cancer Res* 2004; **64**: 523–9.
- 24 Yasui W, Sano T, Nishimura K *et al.* Expression of P-cadherin in gastric carcinomas and its reduction in tumor progression. *Int J Cancer* 1993; **54**: 49–52.
- 25 Alley MC, Scudiero DA, Monks A *et al.* Feasibility of drug screening with panels of human tumor cell lines using a microculture tetrazolium assay. *Cancer Res* 1988; **48**: 589–601.
- 26 Xian CJ, Mardell CE, Read LC. Specificity of the localization of transforming growth factor-alpha immunoreactivity in colon mucosa. *J Histochem Cytochem* 1999; **47**: 949–58.
- 27 Sinicrope FA, Roddey G, Lemoine M *et al.* Loss of p21WAF1/Cip1 protein expression accompanies progression of sporadic colorectal neoplasms but not hereditary nonpolyposis colorectal cancers. *Clin Cancer Res* 1998; **4**: 1251–61.
- 28 Abbas T, Dutta A. p21 in cancer: intricate networks and multiple activities. *Nat Rev Cancer* 2009; **9**: 400–14.
- 29 Park SS, Kang SH, Park JM *et al.* Expression of liver-intestine cadherin and its correlation with lymph node metastasis in gastric cancer: can it predict N stage preoperatively? *Ann Surg Oncol* 2007; **14**: 94–9.
- 30 Ito R, Oue N, Yoshida K *et al.* Clinicopathological significant and prognostic influence of cadherin-17 expression in gastric cancer. *Virchows Arch* 2005; **447**: 717–22.
- 31 Miettinen PJ, Berger JE, Meneses J *et al.* Epithelial immaturity and multiorgan failure in mice lacking epidermal growth factor receptor. *Nature* 1995; **376**: 337–41.
- 32 Barnard JA, Beauchamp RD, Russell WE, Dubois RN, Coffey RJ. Epidermal growth factor-related peptides and their relevance to gastrointestinal pathophysiology. *Gastroenterology* 1995; **108**: 564–80.
- 33 Abud HE, Watson N, Heath JK. Growth of intestinal epithelium in organ culture is dependent on EGF signalling. *Exp Cell Res* 2005; **303**: 252–62.
- 34 Salomon DS, Brandt R, Ciardiello F, Normanno N. Epidermal growth factor-related peptides and their receptors in human malignancies. *Crit Rev Oncol Hematol* 1995; **19**: 183–232.



Olfactomedin-4 is a glycoprotein secreted into mucus in active IBD[☆]

Michael Gersemann^{a, b, *}, Svetlana Becker^b, Sabine Nuding^b, Lena Antoni^b, German Ott^c, Peter Fritz^c, Naohide Oue^d, Wataru Yasui^d, Jan Wehkamp^{a, b}, Eduard F. Stange^a

^a Department of Internal Medicine I, Robert Bosch Hospital, Stuttgart, Germany

^b Dr. Margarete Fischer-Bosch Institute of Clinical Pharmacology, Stuttgart and University of Tübingen, Germany

^c Department of Pathology, Robert Bosch Hospital, Stuttgart, Germany

^d Department of Molecular Pathology, Hiroshima University Graduate School of Biomedical Science, Hiroshima, Japan

Received 12 August 2011; received in revised form 28 September 2011; accepted 28 September 2011

KEYWORDS

Inflammatory bowel disease;
Olfactomedin-4;
Intestinal stem cell marker;
Defensins;
Mucins;
Mucus

Abstract

Background: Olfactomedin-4 (OLFM4) is a glycoprotein characteristic of intestinal stem cells and apparently involved in mucosal defense of the stomach and colon. Here we studied its expression, regulation and function in IBD.

Methods: The expression of OLFM4, mucins Muc1 and Muc2, the goblet cell differentiation factor Hath1 and the proinflammatory cytokine IL-8 was measured in inflamed or noninflamed colon in IBD patients and controls. OLFM4 protein was located by immunohistochemistry, quantified by Dot Blot and its binding capacity to defensins HBD1-3 was investigated. The influence of bacteria with or without the Notch blocker dibenzazepine (DBZ) and of several cytokines on OLFM4 expression was determined in LS174T cells.

Results: OLFM4 mRNA and protein were significantly upregulated in inflamed CD (4.3 and 1.7-fold) and even more pronounced in UC (24.8 and 3.7-fold). OLFM4 expression was correlated to IL-8 but not to Hath1. In controls immunostaining was restricted to the lower crypts but in inflamed IBD it expanded up to the epithelial surface including the mucus. OLFM4 bound to HBD1-3 without profoundly inactivating these defensins. In LS174T-cells OLFM4 mRNA was significantly augmented after incubation with *Escherichia coli* K12, *Escherichia coli* Nissle and *Bacteroides vulgatus*. DBZ downregulated OLFM4 expression and blocked bacterial induction whereas IL-22 but not TNF- α was stimulatory.

[☆] Conference presentation: DDW 2011, Chicago, USA (poster).

* Corresponding author at: Robert Bosch Hospital, Internal Medicine I, Auerbachstr. 110, D-70376 Stuttgart, Germany. Tel.: +49 711 81015912; fax: +49 711 81013793.

E-mail address: michael.gersemann@rbk.de (M. Gersemann).

Conclusions: OLFM4 is overexpressed in active IBD and secreted into mucus. The induction is triggered by bacteria through the Notch pathway and also by the cytokine IL-22. OLFM4 seems to be of functional relevance in IBD as a mucus component, possibly by binding defensins.

© 2011 European Crohn's and Colitis Organisation. Published by Elsevier B.V. All rights reserved.

1. Introduction

In both inflammatory bowel diseases (IBD) the chronic inflammation is mediated by an immune response directed against commensal bacteria, possibly triggered by a disproportionate immune response toward these microbes that damages the mucosa.¹ On the other hand, there is increasing evidence for a primary role of a defective mucosal barrier in Crohn's disease (CD) and ulcerative colitis (UC).^{2–4} Bacteria from the lumen massively contaminate the mucus layer⁵ which is normally sterile in the bottom stratum.⁶ Some bacteria are epithelial adherent^{5,7} or may even invade the sub-epithelial space^{5,8} and thus trigger an immune response.

The mucosal barrier is a multilayer structure composed of the mucus layer⁶ and its origin, the epithelium. In the large intestine the key secretory cells are the goblet cells. They produce various mucins forming the mucus layer which is acting as a physical and chemical barrier against commensals and pathogens.⁹ The colonic epithelium also produces antimicrobial peptides which are ultimately secreted into the mucus.^{10,11} The more important colonic peptides, the β -defensins, are characterized by a broad antimicrobial activity against a variety of gram-positive and gram-negative bacteria preventing luminal microbes to enter the lower mucus layer and attack the epithelium.¹²

This intestinal protective barrier mediated by mucus and defensins is disturbed in IBD. In CD, the expression of the antimicrobial peptides is compromised enabling the bacteria to invade the mucosa and thus trigger inflammation.^{3,13} In case of colonic involvement, CD is linked to a diminished expression of HBD1 independent of inflammation.¹⁴ In UC, the mucus layer is thinner than normal and may even be missing.^{15,16} This is accompanied by a diminished mucin synthesis,^{17–21} which is apparently related to a failure in the differentiation of intestinal stem cells toward goblet cells.¹⁷ This differentiation is governed by the key transcription factor *Hath1* which is correlated with mucin synthesis.¹⁷

Olfactomedin-4 (OLFM4) is an olfactomedin domain-containing protein which was found preferentially in the human gastrointestinal tract.^{22–24} The function of OLFM4 in the digestive tract is probably complex. OLFM4 may be an important part of the gastrointestinal mucosal surface and therefore play a role in its defense.²⁵ For instance, OLFM4 is known to create large polymers stabilized by disulfide bonds,²⁵ similar to mucins.⁹ Moreover, it was demonstrated to interact with cell surface cadherin and lectins facilitating cell adhesion.²⁶ A role of OLFM4 in epithelial defense was concluded from an upregulation in a mouse primary gastric epithelial cell line GSM06 incubated with *Helicobacter pylori*,²⁷ as well as in *H. pylori* infected patients in vivo.²⁸ Finally, in addition to LGR5²⁹ also OLFM4 was found to be a small and large intestinal marker for crypt stem cells in humans.³⁰

However, little is known about its relevance in the colon. Shinozaki et al. found OLFM4 transcripts to be significantly upregulated in the epithelium in active vs. inactive UC but its precise function remained unclear.³¹ In the present study we attempted to better define the role of OLFM4 in the pathogenesis of IBD and suggest that this peptide acts as an inflammation induced mucus component binding defensins.

2. Material and methods

2.1. Patients

The diagnosis of CD and UC was based on classical clinical, radiological and endoscopic findings.^{32,33} Endoscopic biopsies were immediately snap-frozen in liquid nitrogen. All patients gave their written informed consent and the study was approved by the ethical committee of the University of Tübingen (Germany).

For real-time PCR analysis biopsies from the colonic sigma were obtained in a total of 160 individuals, who underwent routine colonoscopy for various indications, such as colon cancer screening, IBD, diarrhea or obstipation. Thirty-three of these biopsies were classified as healthy controls, 72 were from CD patients (36 noninflamed and 36 inflamed samples) and 55 had the diagnosis of UC (28 noninflamed and 27 inflamed samples). All samples were collected at the Robert Bosch Hospital (Stuttgart, Germany) and the intensity of the flare was clinically evaluated in these patients using the Colitis Activity Index (CAI) for UC and the Crohn's disease activity index (CDAI) for CD.

Immunostaining was performed in formalin-fixed or Carnoy-fixed paraffin-embedded colonic tissue. A total of 18 formalin-fixed colonic resections (6 controls, 6 inflamed CD and 6 inflamed UC samples) and 10 Carnoy-fixed rectal biopsies (5 inflamed CD and 5 inflamed UC samples) were investigated. For Dot Blot analysis, sigma biopsies of 4 controls, 4 inflamed CD and 4 inflamed UC patients, as well as mucus extracts obtained by colonoscopic brushings from 3 controls, 3 inflamed CD and 3 inflamed UC samples were collected. Brushings were performed by gently scrubbing the rectal mucosa with an endoscopic brush, removing the endoscope from the rectum and, outside the patient, the brush was cut with scissors and snap frozen in liquid nitrogen.

2.2. RNA isolation and reverse transcription

The frozen tissues were mechanically disrupted and total RNA was isolated using TRIzol reagent (Invitrogen, Karlsruhe, Germany). RNA quality was checked with the Agilent RNA 6000 Nano Kit (Agilent Technologies, Santa Clara, CA, USA). 500 ng of total RNA was reverse transcribed with AMV reverse transcriptase according to the supplier's protocol

(Promega, Mannheim, Germany). RNA preparations were used for real-time PCR analysis.

2.3. Protein preparation

Frozen sigmoid biopsies were pulverized with a pestle in liquid nitrogen. Proteins were extracted under gentle agitation for 90 min diluted in 100 μ l homogenization buffer (50 mM Tris HCl, 250 mM sucrose, 1 mM EDTA, pH 7.6). Extracts were centrifuged for 20 min (13200 g, 4 °C) and the supernatants were immediately snap-frozen in liquid nitrogen. Mucus extracts were incubated for 2 h in 300 μ l 5% acetic acid following a centrifugation for 10 min (7000 g, 4 °C). Then the supernatants were extracted and dried in a vacuum concentrator. Pellets were diluted in 80 μ l 0.01% acetic acid and immediately snap-frozen in liquid nitrogen. Protein content in biopsies and mucus extracts was measured using a Bicinchoninic Acid Protein Assay (Smith) as described previously.³⁴ Isolated proteins were used for Dot Blot analyses.

2.4. Quantitative real-time reverse transcriptase PCR

For mRNA quantification, real-time PCR was carried out in a SYBR Green fluorescence temperature cycler (LightCycler®, Roche Diagnostics, Mannheim, Germany). Single-stranded cDNA (or gene-specific plasmids as controls) corresponding to 10 ng of RNA conducted as a template with specific oligonucleotide primer pairs (Table 1) as described previously.¹³ All primers were tested for specific binding to the sequence of interest using BLAST. Plasmids for each product were generated with the TOPO TA Cloning Kit (Invitrogen, Carlsbad, CA, USA) according to the supplier's protocol. PCR-amplified DNA fragments were confirmed by sequencing. Internal standard curves were produced by serial dilution of the correctly sequenced plasmids. The mRNA data were normalized to β -actin mRNA.

2.5. Immunohistochemistry

A monoclonal antibody directed against OLFM4 (N212) was produced by W.Y. in the Department of Molecular Pathology, Hiroshima University Graduate School of Biomedical Science, Hiroshima, Japan; proof for its specificity has previously been published.³⁵ Immunostaining for OLFM4 was performed using a two-step immunoperoxidase technique (EnVision™, Dako, Glostrup, Denmark) as described previously.³⁶ Antigen retrieval was performed by heating for 30 min in a steamer

(pH 9). Then, sections were incubated for 1 h with the primary anti-OLFM4 antibody diluted 1:100 in TBST (20 mM Tris-Base (pH 7.4), 0.14 M NaCl, 0.1% Tween 20). Visualization was performed using a detection kit as outlined by the supplier (Dako, Glostrup, Denmark: horse-radish-peroxidase (HRP)-labeled secondary antibody, detection with 3'-diaminobenzidine tetrahydrochloride). Sections were counterstained with hematoxylin. The grade of inflammation was blindly evaluated in H & E stained sections by an experienced pathologist blinded to the immunohistochemical and molecular biological results.

2.6. Dot Blot analysis

The specificity of the anti-OLFM4 antibody (N212) was tested in Western Blot experiments using human sigma biopsies. We found a clear signal at 57 kDa in inflamed UC samples which is less intense in inflamed CD and uninflamed controls (data not shown). Due to the limited protein amounts obtained by a single biopsy, we decided to switch to the Dot Blot technique which needs less total protein amounts as compared to the Western Blot. Therefore, 10 μ g of total protein was transferred to 0.45 mg pore size nitrocellulose membranes (Schleicher & Schuell, Keene, NH, USA) and blocked with 5% skimmed milk powder in TBST for 1 h. The membranes were washed and incubated for 1 h with the primary anti-OLFM4 antibody (diluted 1:1000 in 5% skimmed milk powder in TBST). Then, the membranes were washed again and treated for 1 h with the secondary HRP-conjugated goat anti-mouse immunoglobulin G antibody (Immuno Research Laboratories, West Grove, PA, USA; diluted 1:5000 in 5% skimmed milk powder in TBST). Protein detection was performed using the Amersham™ ECL Plus Western Blotting Detection System (GE Healthcare, Chalfont St Giles, UK). Signals were visualized with a chemiluminescence camera charge-coupled device LAS-1000 (Fuji, Tokyo, Japan). Densitometric analysis was performed with AIDA 2.1 software (Raytest, Straubenhardt, Germany).

After 24 h primary and secondary antibodies were removed from the membranes by incubation for 30 min in Restore™ Western Blot Stripping Buffer (Thermo Scientific, Rockford, IL, USA). Then, Dot Blot analysis was performed for β -actin on the same membranes. The primary β -actin antibody (Sigma, Deisenhofen, Germany) and also the secondary HRP-conjugated goat anti-mouse immunoglobulin G antibody (Immuno Research Laboratories, West Grove, PA, USA) were diluted 1:5000 in 5% skimmed milk powder in TBST. Detection of β -actin was performed as described above. In sigma biopsies, OLFM4 protein content was

Table 1 Oligonucleotide primer pairs used for PCR measurements.

Product	Forward primer (5' -> 3')	Reverse primer (5' -> 3')
β -actin	GCCAACCGCGAGAAGATGA	CATCAGATGCCAGTGGTA
IL-8	ATGACTTCCAAGCTGGCCGTGGC	TCTCAGCCCTCTTCAAAAACCTTC
OLFM4	TGCCATTGCGCCGAGAAATCGTGCTCT	TCACCACACCACCATGACCACAGCTCC
Muc1	AGACGTCAGCGTGAGTGATG	CAGCTGCCCGTAGTTCCTTTC
Muc2	ACCCGCACTATGTCAACCTTC	GGGATCGCAGTGGTAGTTGT
Hath1	CGAGAGAGCATCCCGTCTAC	TCCGGGAATGTAGCAAATA

normalized to β -actin by dividing the densitometric intensity (LAU) of OLFM4 through the LAU of β -actin in the same biopsy. Notably, OLFM4 and β -actin, were exposed for the same time period (5 min).

2.7. HBD1-3/OLFM4 binding assay

To investigate the possibility that OLFM4 binds to the major colonic defensins, we developed an HBD1-3/OLFM4 binding assay. Therefore, 96 well plates (Nunc, Roskilde, Denmark) were coated for 3 times in triplicates overnight at 4 °C with 5 μ g HBD1, HBD2 or HBD3 (Peptanova, Sandhausen, Germany) or 5 μ g bovine serum albumin (BSA, Sigma, Deisenhofen, Germany) per well in 100 μ l coating buffer (50 mM NaHCO₃/Na₂CO₃, pH 9.6). As a control, 100 μ l coating buffer alone was used. The next day the wells were washed with TBST and blocked with 5% skimmed milk powder in TBST for 1 h. After repeatedly washing with TBST, the wells were incubated overnight at 4 °C with 0, 2 or 6 μ g OLFM4 (Sino Biological, Beijing, China) in 100 μ l 5% skimmed milk powder in TBST. Then, wells were washed again and incubated with the anti-OLFM4 antibody diluted 1:500 in 5% skimmed milk powder in TBST for 1 h. After repeatedly washing, wells were incubated with a HRP-labeled secondary antibody (Dako, Glostrup, Denmark) for 30 min. Again, wells were washed and thereafter incubated with 200 μ l 2,2'-azino-bis-3-ethylbenzthiazoline-6-sulphonic acid (ABTS, Sigma, Deisenhofen, Germany) for 10 min. Photometric visualization was carried out with Wallac Victor™ 1420 Multilable Counter (Waltham, MA, USA) at 405 nm wave length.

2.8. Flow cytometric assay

Antimicrobial activity was measured with a flow cytometric test as described previously.³⁷ Briefly, suspensions of *Escherichia coli* ATCC 25922 were grown overnight in Schaedler Broth (BD, Sparks, MD, USA) diluted 1:6 with sterile distilled water at 37 °C. Subsequently 1.5 \times 10⁶ mid-logarithmic-phase bacteria/ml in Schaedler Broth 1:6 in a final volume of 100 μ l were incubated with 5 μ g HBD1, HBD2 or HBD3 (Peptanova, Sandhausen, Germany) and 2 or 6 μ g recombinant human OLFM4 (Sino Biological, Beijing, China) at 37 °C. Since OLFM4 is diluted 1 μ g/ μ l in OLFM4-solvent buffer (0.2 μ m filtered solution of PBS, pH 7.4, 3.2% glycerol, 8% trehalose, 8% mannitol) by the company, bacteria were also incubated with 5 μ g HBD1-3 and 2 or 6 μ l OLFM4 solution buffer alone (obtained by the company) for control experiments. Three independent experiments were performed in triplicates. After 90 min, 1 μ g/ml of the membrane potential sensitive dye DiBAC₄(3) (bis-(1,3-dibutylbarbituric acid) trimethine oxonol; Invitrogen, Carlsbad, CA, USA) was added. After 10 min of incubation, the samples were centrifuged for 10 min at 4500 g and the bacterial pellets were resuspended in 300 μ l phosphate buffered saline (pH 7.4). With a FACSCalibur™ flow cytometer (BD, Sparks, MD, USA) 10 000 events of each sample were analyzed for light scattering and green fluorescence. Antimicrobial activity was determined as percentage of fluorescent depolarized bacteria.

2.9. Cell culture experiments

The colon adenocarcinoma cell line LS174T (American Type Culture Collection, Manassas, USA) was cultivated in Dulbecco's modified Eagle medium (DMEM, Gibco Life Technologies, Eggenstein, Germany) completed with 10% fetal calf serum (FCS, PAA Laboratories, Pasching, Austria), 1% non essential amino acids (Gibco Life Technologies, Eggenstein, Germany), 1% penicillin/streptomycin (Gibco Life Technologies, Eggenstein, Germany) and 1% sodium pyruvate (Gibco Life Technologies, Eggenstein, Germany) in a humidified atmosphere at 37 °C and 5% CO₂. For experiments, cells were seeded for at least 3 times in triplicates into 12-well culture plates (Becton Dickinson, Franklin Lakes, New Jersey, USA) at a density of 0.65 \times 10⁶ per well. At about 70% confluence, cells were washed with phosphate-buffered saline (Gibco Life Technologies, Eggenstein, Germany) and incubated in FCS- and antibiotic-free DMEM for 12 h.

Then, cells were incubated with *E. coli* K12, *E. coli* Nissle, *Bacteroides vulgatus*, *Symbioflor G1/G2/G3*, *Lactobacillus fermentum* and *acidophilus*, as well as *Bifidobacterium longum*, *breve* and *adolescentis* for 6 and 24 h. All *E. coli* strains and *B. vulgatus* were cultivated under aerobic, *Lactobacilli* and *Bifidobacteria* under anaerobic conditions as previously described.³⁸ Bacteria were killed per heat inactivation in a water bath at 65 °C for 1 h. Then, bacteria were washed with PBS and adjusted to a density of 3 \times 10⁸ cells/ml with FCS- and antibiotic-free DMEM. To investigate the possible role of the Notch signaling pathway in regulating OLFM4, cells were incubated for 6 and 24 h with the γ -secretase inhibitor dibenzazepine (DBZ, Axon Medchem, Groningen, Netherlands) in a concentration of 1 μ M (in 0.1% DMSO in DMEM) in the absence or presence of *E. coli* Nissle. LS174T cells were also treated with 10 ng/ml TNF- α (Sigma, Deisenhofen, Germany), 100 ng/ml IL-22 (Sigma, Deisenhofen, Germany), 10 ng/ml IL-4 (Sigma, Deisenhofen, Germany) and 10 ng/ml IL-13 (Sigma, Deisenhofen, Germany) for 6, 12 and 24 h. At the end of experiments cells were washed with PBS and mRNA was isolated using RNeasy Mini Kit (Qiagen, Venlo, Netherlands) according to the supplier's protocol.

2.10. Statistics

Statistical analyses were performed and all graphs were generated with the GraphPad Prism version 4.0 software using the Mann-Whitney test. In case of the PCR measurements in human sigma biopsies, Bonferroni correction was also done. Spearman's rank analysis was performed for nonparametric correlation between the different subgroups of the quantitative real-time PCR results. Values of $p < 0.05$ were considered to be statistically significant. Data are presented in box and whiskers (means).

3. Results

3.1. OLFM4 and mucins are differentially expressed in inflamed IBD

In colonic biopsies transcripts of the proinflammatory cytokine IL-8 (Fig. 1A) were equally enhanced in inflamed CD

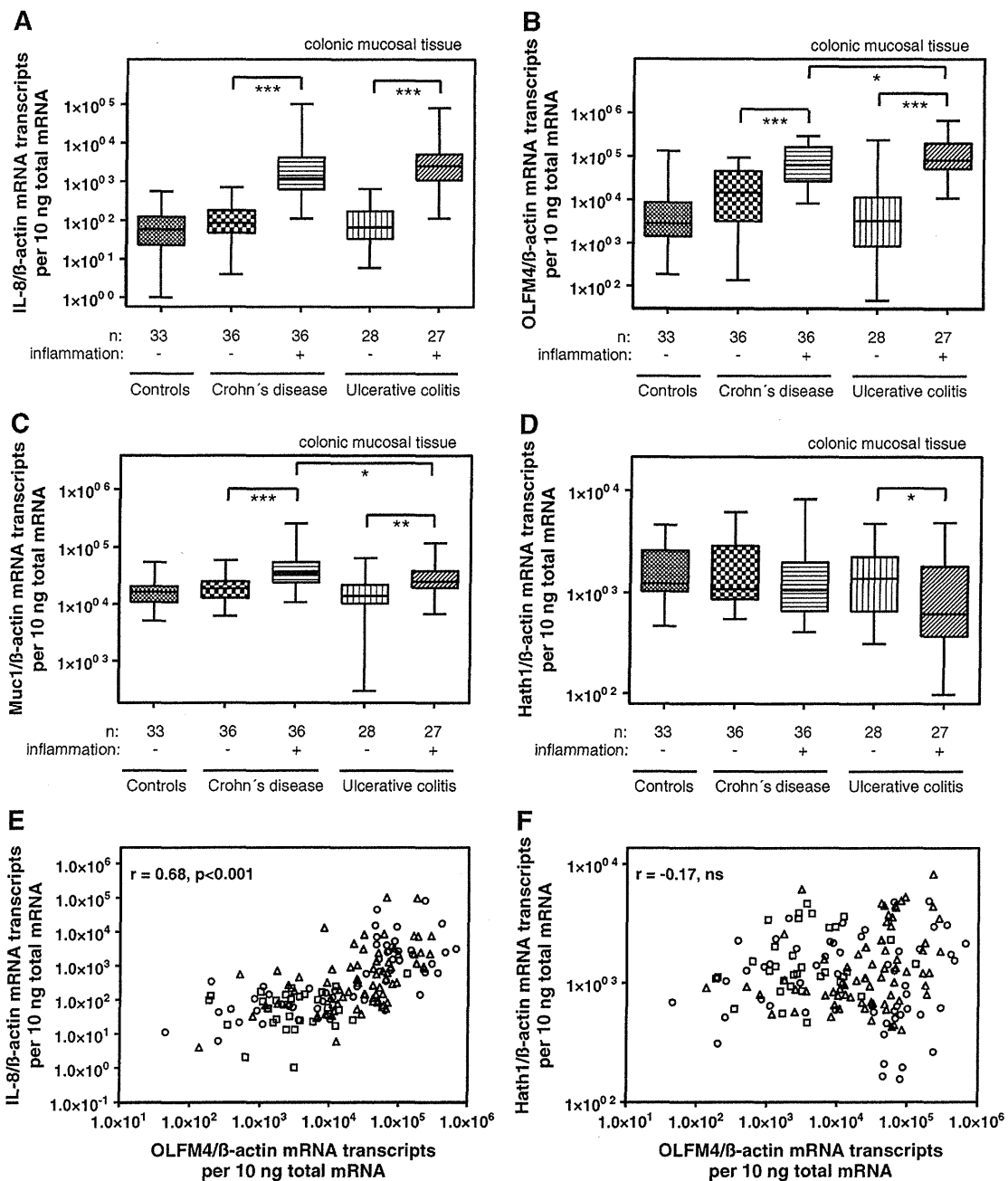


Figure 1 IL-8, OLFM4, Muc1 and Hath1 expression in controls and IBD mucosa: IL-8 transcripts are enhanced in inflamed vs. noninflamed CD and UC without significant differences between both diseases (A). OLFM4 mRNA was significantly more induced in UC than CD (B). Muc1 transcripts are augmented more in inflamed vs. noninflamed CD than in UC (C). Hath1 mRNA is significantly downregulated in inflamed UC (D). OLFM4 is highly correlated with IL-8 (E, $r = 0.68$ for all samples, $p < 0.001$) but not with Hath1 (F, $r = -0.17$ for all samples, ns; squares = controls, triangles = CD, circles = UC; *, $p < 0.05$ (these significances are lost after Bonferroni correction), **, $p < 0.01$, ***, $p < 0.001$).

(14-fold, $p < 0.001$) and UC (38-fold, $p < 0.001$) compared to the respective noninflamed samples. In controls and noninflamed IBD samples IL-8 expression was comparably low. The grade of histological inflammation was similar in both inflamed IBD entities (inflammation score for controls: 1.0, for CD: 7.2 and for UC: 7.0). The CAI was 2.6 for the

noninflamed UC group and 12.1 for the inflamed UC patients. The CDAI was 188 in case of noninflamed colonic CD and 237 in inflamed colonic CD patients.

OLFM4 mRNA (Fig. 1B) was significantly induced in inflamed CD (4.3-fold, $p < 0.001$) and UC (24.8-fold, $p < 0.001$) vs. noninflamed biopsies. This upregulation was clearly

higher in inflamed UC than in inflamed CD samples (5.8-fold, $p=0.04$). Again, controls and noninflamed samples were in the same range. Immunostaining for OLFM4 in normal human colonic tissues was confined to the lower third of crypts but expanded during inflammation up to the epithelial surface (Fig. 2). The OLFM4 protein content normalized to β -actin as determined by Dot Blot analysis (Fig. 3) was also clearly augmented in inflamed CD (1.7-fold, $p=0.03$) and UC (3.7-fold, $p=0.03$) as compared to controls. Again, this induction was numerically more pronounced in inflamed UC as compared to inflamed CD (ns).

Muc1 transcripts (Fig. 1C) were also significantly augmented in inflamed CD (1.9-fold, $p<0.001$) and UC (1.8-fold, $p=0.002$) samples as compared to controls. In contrast to OLFM4, this induction was less significant in inflamed UC

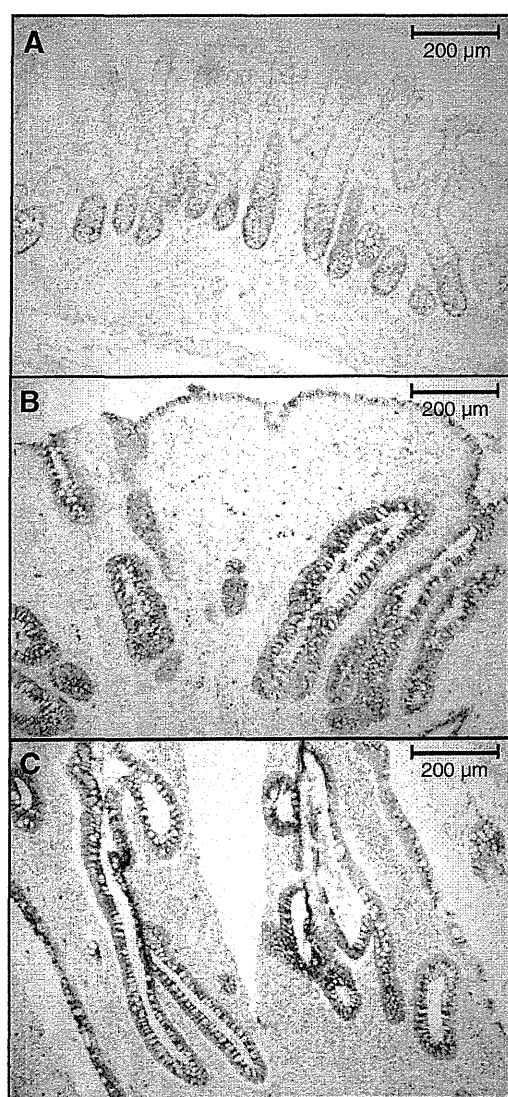


Figure 2 OLFM4 immunostaining in controls and IBD mucosa: OLFM4 staining is located in the lower third of the crypt in control samples (A, magnification 100-fold) and expanded up to the epithelial surface during inflammation (B = inflamed CD, C = inflamed UC, magnification 100-fold).

than in inflamed CD biopsies ($p=0.03$). Controls and noninflamed samples exhibited a comparable expression. Muc2 mRNA levels did not show significant differences between the 5 subgroups (data not shown). Hath1 expression (Fig. 1D) was significantly lower in inflamed vs. noninflamed UC (0.7-fold, $p=0.02$) but not CD. Transcripts of OLFM4 correlated significantly with IL-8 (Spearman $r: 0.68$, $p<0.001$, Fig. 1E) and Muc1 ($r: 0.57$, $p<0.001$) but not with Hath1 ($r: -0.17$, ns, Fig. 1F).

3.2. OLFM4 is secreted into the mucus and binds to β -defensins HBD1-3

Since OLFM4 is upregulated in inflamed IBD and staining was found up to the epithelial surface, we searched for OLFM4 protein in human mucus following Carnoy-fixation. Indeed, rectal IBD biopsies showed a positive immunostaining for OLFM4 in the crypt lumen (Fig. 4A) as well as in the surface mucus (Fig. 4B), implying the secretion of OLFM4 by epithelial cells into the mucus. This observation was confirmed in rectal mucus extracts, which were obtained by colonoscopic brushings and analyzed with the Dot Blot technique (Fig. 4C): OLFM4 protein was found in the mucus of patients with inflamed CD and even more pronounced in patients with inflamed UC, whereas noninflamed mucus controls were almost negative. As expected, β -actin was only marginally detectable in mucus showing that these extracts were almost free of cell detritus.

The defensins HBD1-3 are positively charged and also secreted into the mucus¹⁰ whereas OLFM4 has a negative charge. Therefore, we tested the ability of recombinant OLFM4 to bind HBD1-3 preabsorbed to plastic wells. In contrast to no binding to BSA, OLFM4 preferentially bound to preabsorbed HBD3>HBD2 and >HBD1 (Fig. 5). Next, we checked the antimicrobial activity of HBD1-3 in the absence and presence of OLFM4. The coincubation of defensins with OLFM4 at 2 and 6 $\mu\text{g}/\text{ml}$ was associated with a limited reduction of the antimicrobial activity in case of HBD1 from 66% to 58% (2 $\mu\text{g}/\text{ml}$, ns) and 47% to 39% (6 $\mu\text{g}/\text{ml}$, ns), in case of HBD2 from 69% to 54% (2 $\mu\text{g}/\text{ml}$, ns) and from 57% to 41% (6 $\mu\text{g}/\text{ml}$, ns) and in case of HBD3 from 71% to 65% (2 $\mu\text{g}/\text{ml}$, ns) and from 55% to 51% (6 $\mu\text{g}/\text{ml}$, ns).

3.3. Bacteria and IL-22 induce OLFM4 expression in LS174T cells

The mucin producing colon adenocarcinoma cell line LS174T was incubated with heat killed *E. coli* K12, *E. coli* Nissle, *B. vulgatus*, *Symbioflor* G1/G2/G3, *L. fermentum* and *acidophilus*, as well as *B. longum*, *breve* and *adolescentis*. An incubation for 24 h with *E. coli* K12 (2.8-fold induction, $p=0.009$), *E. coli* Nissle (2.5-fold, $p=0.02$) and *B. vulgatus* (1.9-fold, $p=0.02$) led to a significant increase of OLFM4 expression in these LS174T cells. In contrast, OLFM4 was unaffected by heat killed *Symbioflor* G1/G2/G3, *L. fermentum* and *acidophilus*, as well as *B. longum*, *breve* and *adolescentis* (data not shown).

In addition, LS174T cells showed a significant time-dependent increase of OLFM4 expression following a treatment with 100 ng/ml IL-22 (3.4-fold after 6 h, $p=0.04$; 5.3-fold after 12 h, $p=0.01$; 9.1-fold after 24 h, $p=0.01$). In

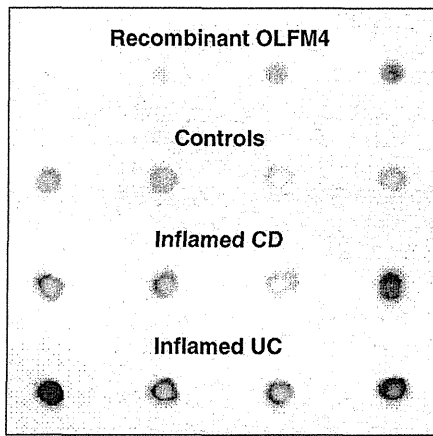


Figure 3 OLFM4 Dot Blot analysis in controls and IBD mucosa: OLFM4 protein is significantly increased in inflamed CD and even more pronounced in inflamed UC biopsy samples as compared to controls (top lane: recombinant OLFM4 in increasing amounts from left to right: 0.05, 0.1, 0.5 and 1 µg).

contrast, incubation with TNF-α (0.8–1.4-fold increase, ns), IL-4 (0.7–1.0-fold, ns) and IL-13 (0.7–1.3-fold, ns) did not influence OLFM4 expression.

3.4. OLFM4 is regulated by the Notch pathway

To elucidate the mechanism by which bacteria can influence the level of OLFM4 expression, we investigated the involvement of the Notch pathway in the regulation of OLFM4. Accordingly, LS174T cells were treated with heat inactivated *E. coli Nissle* in the presence or absence of γ-secretase inhibitor dibenzazepine (DBZ, Fig. 6). In the absence of

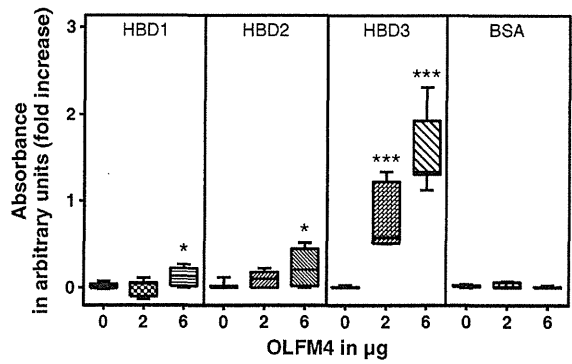


Figure 5 OLFM4 binding to HBD1-3: Coincubation of OLFM4 with HBD1-3, but not bovine serum albumin (BSA), resulted in a dose dependent increase of OLFM4 absorption (*: p<0.05, ***: p<0.001).

bacteria DBZ treatment resulted in a significant downregulation of OLFM4 transcripts to 11% after 24 h (p=0.004). The coincubation with *E. coli Nissle* and DBZ for 24 h nearly completely blocked the 2.4 fold induction by *E. coli Nissle* (p=0.004).

4. Discussion

OLF4 is still an enigmatic, ambiguous protein. On the one hand, the protein marks intestinal stem cells,³⁰ on the other hand it also seems to be important in host defense during gastric and colonic infection and inflammation.^{25–27} In particular, the regulation and function of OLF4 in the colon are still not completely understood.²⁵

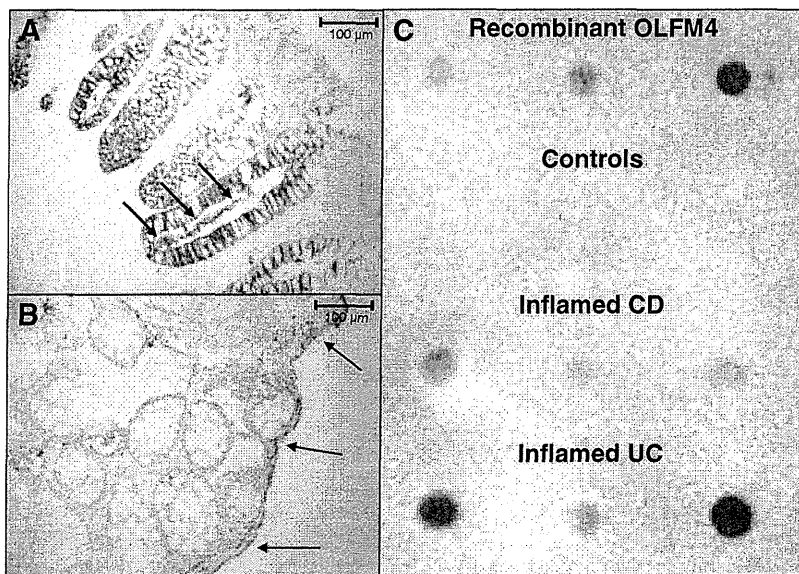


Figure 4 Secreted OLFM4 in controls and IBD mucus: OLFM4 is found in the crypt lumen (A = CD, arrows, magnification 200-fold) and also in the surface mucus (B = UC, arrows, magnification 200-fold). Dot Blot analysis demonstrates OLFM4 in rectal mucus extracts (C, top lane: recombinant OLFM4 in increasing concentrations from left to right: 0.05, 0.1 and 0.5 µg).

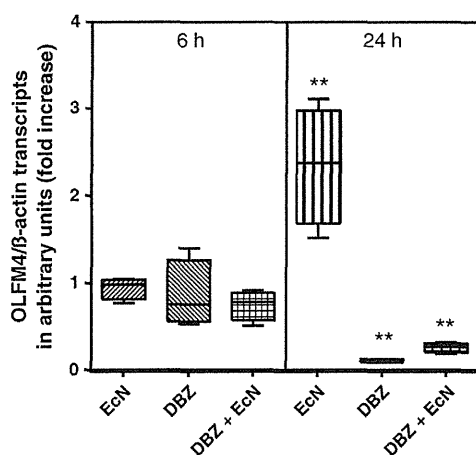


Figure 6 OLFM4 expression in LS174T cells incubated with *E. coli Nissle* (EcN) in the presence and absence of the γ -secretase inhibitor dibenzazepine (DBZ). 24 h of incubation with EcN led to a significant increase of OLFM4 transcripts. Treatment with DBZ led to a significant downregulation of OLFM4 transcripts after 24 h. DBZ blocked the stimulation by EcN. Values are compared to controls at the given time-point set to 1 (*: $p < 0.05$, **: $p < 0.01$). This experiment was performed for 4 times in triplicates.

The current study shows that OLFM4 transcripts and also protein are significantly induced in colonic IBD during inflammation. Moreover, OLFM4 expression correlates significantly with that of the proinflammatory cytokine IL-8, but not with the goblet cell differentiation factor Hath1. This implies that OLFM4 expression is triggered by inflammation and not by differentiation, in contrast to mucins.¹⁷ The relative induction of OLFM4 is clearly higher in active UC compared to active CD. In principle, this observation is consistent with the observation of Shinozaki and his group, who found OLFM4 mRNA to be elevated in active vs. inactive UC.³¹

In healthy controls, we found OLFM4 staining to be located primarily in the lower third of the colonic crypt, suggesting that in healthy gut this glycoprotein is not a relevant protective factor in the surface epithelium and mucus. However, during active inflammation OLFM4 immunostaining expanded up to the epithelial surface in IBD samples. Shinozaki et al. detected OLFM4 mRNA signals confined to the crypt epithelial cells by in situ hybridization³¹ whereas Clevers and his group³⁰ found colonic OLFM4 mRNA in humans even restricted to crypt base columnar cells again by in-situ hybridization. It seems possible that in controls the protein expression is retained also in stem cell derived daughter cells colonizing the lower third of the crypt, whereas during inflammation the epithelial cells expressing the protein migrate rapidly up to the surface³⁹ where it is secreted. This was evident from the presence of OLFM4 protein in the mucus of Carnoy-fixed IBD biopsies, as well as in rectal IBD mucus obtained by endoscopic brushings. Notably, Dot Blot of these mucus extracts was almost free of β -actin implying that the mucus was not significantly contaminated by cell detritus. The high amino acid sequence similarity between OLFM4 and olfactomedin,²³ the first member of the olfactomedin domain-containing family found to be expressed in the extracellular

mucus matrix of olfactory neuroepithelium in bullfrogs,^{40–42} also underlines the fate of OLFM4 as a secretory protein.

Moreover, we measured the expression of OLFM4 in relation to the two crucial mucins Muc1 and Muc2. In contrast to unchanged Muc2, Muc1 was induced in both diseases, although somewhat less significant in UC. This is consistent with prior observations showing a compromised mucin synthesis in UC.^{17–20} Interestingly, this induction pattern contrasts with OLFM4 expression, which showed a higher induction in UC. It is therefore possible that OLFM4 acts as a mucin substitute complementing the mucus layer during inflammation and bacterial attack.

Since OLFM4 is negatively and HBD1-3 positively charged, binding is probably electrostatic. Both defensins¹⁰ and OLFM4 are located in the mucus, therefore it is plausible that they interact and bind to each other also in vivo in order to concentrate the antimicrobial activity in the mucus. Notably, OLFM4 led only to a minor reduction of the antimicrobial activity of HBD1, HBD2 and HBD3. Thus, OLFM4 appears to function as a glycoprotein binding but not profoundly inactivating defensins. However, it should be noted that recombinant OLFM4 differs from native OLFM4 with respect to its glycosylation.

In addition, we observed OLFM4 transcripts to be induced in LS174T cells after incubation with heat killed *E. coli* K12, *E. coli Nissle* and *B. vulgatus*. Although this is the first description in colonic cells, the principle that specific bacteria may enhance OLFM4 expression was previously demonstrated in the mouse primary gastric epithelial cell line GSM06 incubated with *H. pylori*.²⁷ Even more pronounced was the induction by IL-22, a susceptibility gene in UC,⁴³ also compared to the other cytokines tested. The induction of OLFM4 as a mucus glycoprotein is consistent with the recent observation of an IL-22 mediated increase in goblet cell counts and mucin synthesis in experimental animals.⁴⁴ This cytokine also increases the innate immunity of several tissues by the induction of antimicrobial peptides such as HBD2 and HBD3.⁴⁵ Accordingly, IL-22 was demonstrated to protect mice from colitis,⁴⁶ probably by enhancing the mucus/defensin barrier.

Gene expression profiling experiments found OLFM4 to be a target gene of the Notch pathway and thus cell differentiation, proliferation, and immune response to inflammation.⁴⁷ We confirmed this observation by cell culture experiments showing that treatment of LS174T cells with the γ -secretase inhibitor DBZ led to a significant downregulation of OLFM4 transcripts. Moreover, the *E. coli Nissle* mediated induction was also blocked by DBZ, pointing out that the bacterial triggered OLFM4 induction depends on the Notch pathway.

In summary, OLFM4 possesses several "mucin-like" properties (negatively charged polymerizing glycoprotein, secreted into mucus, binding to defensins) and is extensively upregulated in inflamed IBD mucosa where it expands up to the surface epithelium and is secreted into the mucus. The induction may be mediated by bacteria via the Notch pathway and through IL-22. OLFM4 is suggested to have a functional protective role in IBD by binding defensins in the mucus.

Conflict of interest

All Authors have no conflict of interest.

Acknowledgment

The scientific input by Robert Küchler and the technical help by Nadine Krüger, Jutta Bader, Marion Schiffmann, Dagmar Weller, Michelle Katajew, and Kathleen Siegel are gratefully acknowledged.

This research work is supported by the Robert Bosch Foundation, Stuttgart, Germany and the Emmy Noether program (J.W.) of the Deutsche Forschungsgemeinschaft (DFG).

References

- Sartor RB. Microbial influences in inflammatory bowel diseases. *Gastroenterology* 2008;134:577–94.
- Schreiber S, Rosenstiel P, Albrecht M, Hampe J, Krawczak M. Genetics of Crohn disease, an archetypal inflammatory barrier disease. *Nat Rev Genet* 2005;6:376–88.
- Gersemann M, Wehkamp J, Fellermann K, Stange EF. Crohn's disease—defect in innate defence. *World J Gastroenterol* 2008;14:5499–503.
- Gersemann M, Stange EF, Wehkamp J. From intestinal stem cells to inflammatory bowel diseases. *World J Gastroenterol* 2011;17:3198–203.
- Swidsinski A, Weber J, Loening-Baucke V, Hale LP, Lochs H. Spatial organization and composition of the mucosal flora in patients with inflammatory bowel disease. *J Clin Microbiol* 2005;43:3380–9.
- Johansson ME, Larsson JM, Hansson GC. The two mucus layers of colon are organized by the MUC2 mucin, whereas the outer layer is a legislator of host–microbial interactions. *Proc Natl Acad Sci U S A* 2011;108(Suppl 1):4659–65.
- Darfeuille-Michaud A, Neut C, Barnich N, Lederman E, Di Martino P, Desreumaux P, et al. Presence of adherent *Escherichia coli* strains in ileal mucosa of patients with Crohn's disease. *Gastroenterology* 1998;115:1405–13.
- Moussata D, Goetz M, Gloeckner A, Kerner M, Campbell B, Hoffman A, et al. Confocal laser endomicroscopy is a new imaging modality for recognition of intramucosal bacteria in inflammatory bowel disease in vivo. *Gut* 2011;60:26–33.
- Shirazi T, Longman RJ, Corfield AP, Probert CS. Mucins and inflammatory bowel disease. *Postgrad Med J* 2000;76:473–8.
- Meyer-Hoffert U, Hornef MW, Henriques-Normark B, Axelsson LG, Midtvedt T, Pütsep K, et al. Secreted enteric antimicrobial activity localises to the mucus surface layer. *Gut* 2008;57:764–71.
- Wehkamp J, Schmid M, Fellermann K, Stange EF. Defensin deficiency, intestinal microbes, and the clinical phenotypes of Crohn's disease. *J Leukoc Biol* 2005;77:460–5.
- Wehkamp J, Schmid M, Stange EF. Defensins and other antimicrobial peptides in inflammatory bowel disease. *Curr Opin Gastroenterol* 2007;23:370–8.
- Wehkamp J, Harder J, Weichenthal M, Mueller O, Herrlinger KR, Fellermann K, et al. Inducible and constitutive beta-defensins are differentially expressed in Crohn's disease and ulcerative colitis. *Inflamm Bowel Dis* 2003;9:215–23.
- Peyrin-Biroulet L, Beisner J, Wang G, Nuding S, Oommen ST, Kelly D, et al. Peroxisome proliferator-activated receptor gamma activation is required for maintenance of innate antimicrobial immunity in the colon. *Proc Natl Acad Sci U S A* 2010;107:8772–7.
- McCormick DA, Horton LW, Mee AS. Mucin depletion in inflammatory bowel disease. *J Clin Pathol* 1990;43:143–6.
- Pullan RD, Thomas GA, Rhodes M, Newcombe RG, Williams GT, Allen A, et al. Thickness of adherent mucus gel on colonic mucosa in humans and its relevance to colitis. *Gut* 1994;35:353–9.
- Gersemann M, Becker S, Kubler I, Koslowski M, Wang G, Herrlinger KR, et al. Differences in goblet cell differentiation between Crohn's disease and ulcerative colitis. *Differentiation* 2009;77:84–94.
- Hanski C, Born M, Foss HD, Marowski B, Mansmann U, Arastéh K, et al. Defective post-transcriptional processing of MUC2 mucin in ulcerative colitis and in Crohn's disease increases detectability of the MUC2 protein core. *J Pathol* 1999;188:304–11.
- Moehle C, Ackermann N, Langmann T, Aslanidis C, Kel A, Kel-Margoulis O, et al. Aberrant intestinal expression and allelic variants of mucin genes associated with inflammatory bowel disease. *J Mol Med* 2006;84:1055–66.
- Tytgat KM, van der Wal JW, Einerhand AW, Büller HA, Dekker J. Quantitative analysis of MUC2 synthesis in ulcerative colitis. *Biochem Biophys Res Commun* 1996;224:397–405.
- Van Klinken BJ, van der Wal JW, Einerhand AW, Büller HA, Dekker J. Sulphation and secretion of the predominant secretory human colonic mucin MUC2 in ulcerative colitis. *Gut* 1999;44:387–93.
- Liu W, Zhu J, Cao L, Rodgers GP. Expression of hGC-1 is correlated with differentiation of gastric carcinoma. *Histopathology* 2007;51:157–65.
- Zhang J, Liu WL, Tang DC, Chen L, Wang M, Pack SD, et al. Identification and characterization of a novel member of olfactomedin-related protein family, hGC-1, expressed during myeloid lineage development. *Gene* 2002;283:83–93.
- Zhang X, Huang Q, Yang Z, Li Y, Li CY. GW112, a novel antiapoptotic protein that promotes tumor growth. *Cancer Res* 2004;64:2474–81.
- Grover PK, Hardingham JE, Cummins AG. Stem cell marker olfactomedin 4: critical appraisal of its characteristics and role in tumorigenesis. *Cancer Metastasis Rev* 2010;29:761–75.
- Liu W, Chen L, Zhu J, Rodgers GP. The glycoprotein hGC-1 binds to cadherin and lectins. *Exp Cell Res* 2006;312:1785–97.
- Liu W, Yan M, Liu Y, Wang R, Li C, Deng C, et al. Olfactomedin 4 down-regulates innate immunity against *Helicobacter pylori* infection. *Proc Natl Acad Sci U S A* 2010;107:11056–61.
- Mannick EE, Schurr JR, Zapata A, Lentz JJ, Gastanaduy M, Cote RL, et al. Gene expression in gastric biopsies from patients infected with *Helicobacter pylori*. *Scand J Gastroenterol* 2004;39:1192–200.
- Barker N, van Es JH, Kuipers J, Kujala P, van den Born M, Cozijnsen M, et al. Identification of stem cells in small intestine and colon by marker gene Lgr5. *Nature* 2007;449:1003–7.
- van der Flier LG, Haegebarth A, Stange DE, van de Wetering M, Clevers H. OLFM4 is a robust marker for stem cells in human intestine and marks a subset of colorectal cancer cells. *Gastroenterology* 2009;137:15–7.
- Shinozaki S, Nakamura T, Iimura M, Kato Y, Iizuka B, Kobayashi M, et al. Upregulation of Reg 1alpha and GW112 in the epithelium of inflamed colonic mucosa. *Gut* 2001;48:623–9.
- Stange EF, Travis SP, Vermeire S, Reinisch W, Geboes K, Barakauskiene A, et al. European evidence-based consensus on the diagnosis and management of ulcerative colitis: definitions and diagnosis. *J Crohns Colitis* 2008;2:1–23.
- Van Assche G, Dignass A, Panes J, Beaugerie L, Karagiannis J, Allez M, et al. The second European evidence-based consensus on the diagnosis and management of Crohn's disease: definitions and diagnosis. *J Crohns Colitis* 2010;4:7–27.
- Stoscheck CM. Quantitation of protein. *Methods Enzymol* 1990;182:50–68.
- Oue N, Sentani K, Noguchi T, Ohara S, Sakamoto N, Hayashi T, et al. Serum olfactomedin 4 (GW112, hGC-1) in combination with Reg IV is a highly sensitive biomarker for gastric cancer patients. *Int J Cancer* 2009;125:2383–92.
- Schmid M, Fellermann K, Fritz P, Wiedow O, Stange EF, Wehkamp J. Attenuated induction of epithelial and leukocyte serine anti-proteases elafin and secretory leukocyte protease inhibitor in Crohn's disease. *J Leukoc Biol* 2007;81:907–15.
- Nuding S, Fellermann K, Wehkamp J, Mueller HA, Stange EF. A flow cytometric assay to monitor antimicrobial activity of

- defensins and cationic tissue extracts. *J Microbiol Methods* 2006;**65**:335–45.
38. Schlee M, Harder J, Kolen B, Stange EF, Wehkamp J, Fellermann K. Probiotic lactobacilli and VSL#3 induce enterocyte beta-defensin 2. *Clin Exp Immunol* 2008;**151**:528–35.
 39. Serafini EP, Kirk AP, Chambers TJ. Rate and pattern of epithelial cell proliferation in ulcerative colitis. *Gut* 1981;**22**:648–52.
 40. Bal RS, Anholt RR. Formation of the extracellular mucous matrix of olfactory neuroepithelium: identification of partially glycosylated and nonglycosylated precursors of olfactomedin. *Biochemistry* 1993;**32**:1047–53.
 41. Snyder DA, Rivers AM, Yokoe H, Menco BP, Anholt RR. Olfactomedin: purification, characterization, and localization of a novel olfactory glycoprotein. *Biochemistry* 1991;**30**:9143–53.
 42. Yokoe H, Anholt RR. Molecular cloning of olfactomedin, an extracellular matrix protein specific to olfactory neuroepithelium. *Proc Natl Acad Sci U S A* 1993;**90**:4655–9.
 43. Silverberg MS, Cho JH, Rioux JD, McGovern DP, Wu J, Annese V, et al. Ulcerative colitis-risk loci on chromosomes 1p36 and 12q15 found by genome-wide association study. *Nat Genet* 2009;**41**:216–20.
 44. Sugimoto K, Ogawa A, Mizoguchi E, Shimomura Y, Andoh A, Bhan AK, et al. IL-22 ameliorates intestinal inflammation in a mouse model of ulcerative colitis. *J Clin Invest* 2008;**118**:534–44.
 45. Wolk K, Kunz S, Witte E, Friedrich M, Asadullah K, Sabat R. IL-22 increases the innate immunity of tissues. *Immunity* 2004;**21**:241–54.
 46. Zenewicz LA, Yancopoulos GD, Valenzuela DM, Murphy AJ, Stevens S, Flavell RA. Innate and adaptive interleukin-22 protects mice from inflammatory bowel disease. *Immunity* 2008;**29**:947–57.
 47. Rodilla V, Villanueva A, Obrador-Hevia A, Robert-Moreno A, Fernández-Majada V, Grilli A, et al. Jagged1 is the pathological link between Wnt and Notch pathways in colorectal cancer. *Proc Natl Acad Sci U S A* 2009;**106**:6315–20.

Upregulation of HOXA10 in gastric cancer with the intestinal mucin phenotype: reduction during tumor progression and favorable prognosis

Kazuhiro Sentani, Naohide Oue, Yutaka Naito, Naoya Sakamoto, Katsuhiko Anami, Htoo Zarni Oo, Naohiro Uraoka, Kazuhiko Aoyagi¹, Hiroki Sasaki¹ and Wataru Yasui*

Department of Molecular Pathology, Hiroshima University Graduate School of Biomedical Sciences, Hiroshima, Japan and ¹Division of Genetics, National Cancer Center Research Institute, Tokyo, Japan

*To whom correspondence should be addressed. Tel: +81 82 257 5145; Fax: +81 82 257 5149; Email: wyasui@hiroshima-u.ac.jp

Gastric cancer (GC) is one of the most common malignancies worldwide. Better knowledge of the changes in gene expression that occur during gastric carcinogenesis may lead to improvements in diagnosis, treatment and prevention. In this study, we screened for genes upregulated in GC by comparing gene expression profiles from microarray and serial analysis of gene expression and identified the *HOXA10* gene. The aim of the present study was to investigate the significance of *HOXA10* in GC. Immunohistochemical analysis demonstrated that 221 (30%) of 749 GC cases were positive for *HOXA10*, whereas *HOXA10* was scarcely expressed in non-neoplastic gastric mucosa except in the case of intestinal metaplasia. Next, we analyzed the relationship between *HOXA10* expression and clinicopathological characteristics. *HOXA10* expression showed a significant inverse correlation with the depth of invasion and was observed more frequently in the differentiated type of GC than in the undifferentiated type of GC. *HOXA10* expression was associated with GC with the intestinal mucin phenotype and correlated with *CDX2* expression. Furthermore, the prognosis of patients with positive *HOXA10* expression was significantly better than in the negative expression cases. 3-(4,5-dimethylthiazole-2-yl)-2,5-diphenyl tetrazolium bromide and wound healing assay revealed that knockdown of *HOXA10* in GC cells by short interfering RNA transfection significantly increased viability and motility relative to the negative control, indicating that *HOXA10* expression inhibits cell growth and motility. These results suggest that expression of *HOXA10* may be a key regulator for GC with the intestinal mucin phenotype.

Introduction

Gastric cancer (GC) is one of the most common human cancers. Cancer develops as a result of multiple genetic and epigenetic alterations (1). Better knowledge of the changes in gene expression that occur during gastric carcinogenesis may lead to improvements in diagnosis, treatment and prevention. Identification of novel biomarkers for cancer diagnosis and novel targets for treatment are major goals in this field (2). We previously performed several large-scale gene expression studies using array-based hybridization (3), serial analysis of gene expression (SAGE) (4,5) and the *Escherichia coli* ampicillin secretion trap (CAST) method (6) and identified several genes including *regenerating islet-derived family, member 4* (*REG4*, which encodes REG IV) (7,8), *palate, lung and nasal epithelium carcinoma-associated protein* (*PLUNC*) (9), *GJB6* (encoding connexin 30) (10) and *DSC2* (encoding desmocollin 2) (11). These results indicated that these methods are useful for identification of novel genes associated with GC; however, such alterations cannot completely explain the pathogenesis of GC. In

Abbreviations: cDNA, complementary DNA; GC, gastric cancer; RT-PCR, reverse transcription-PCR; SAGE, serial analysis of gene expression; siRNA, short interfering RNA.

our previous study, the 20 genes showing the greatest increase in expression on the microarray were quite different from those obtained by SAGE (9). Therefore, we performed gene expression profiling using Affymetrix GeneChip arrays of GC samples previously analyzed by SAGE and identified several candidate GC-associated genes. Among these candidate genes, the *homeobox A10* (*HOXA10*) gene is upregulated in all samples. To date, little is known about the role of *HOXA10* in human GC.

The *HOX* genes are important regulators of embryonic morphogenesis and differentiation and control normal development patterning along the anteroposterior axis. They contain a common DNA motif of a sequence of 183 nucleotides, encoding a region of 61 amino acids called the homeodomain, their sequences being the basis for classification into different subsets (12). The homeodomain is responsible for recognizing and binding to sequence-specific DNA motifs and cis regulates the transcription of genes relevant to the formation of specific segmental architecture. In humans, 38 *HOX*s have been identified that are spread among four different clusters located on four separate chromosomes: 7 (*HOXA*), 17 (*HOXB*), 12 (*HOXC*) and 2 (*HOXD*) (13). A putative role of *HOX*s in malignant processes has been well documented in leukemia. They participate in myeloid cell differentiation and proliferation (14,15). *HOXA10* and *HOXA9* are associated with acute myeloid leukemia and mixed lineage leukemia fusion genes (16). *HOXA10* controls uterine organogenesis during embryonic development and endometrial differentiation in adults (17). Deregulation of *HOXA10* correlates with progression of endometrial carcinoma (18). *CDX2* has been reported to be an upstream regulator for *HOXA10* in myeloid cells and participates in leukemogenesis (19). However, the exact pathogenic mechanisms associated with *HOXA10* in stomach carcinogenesis remain obscure.

The present study represents the first detailed analysis of *HOXA10* expression in GC. To clarify the pattern of expression and localization of *HOXA10* in GC, we performed immunohistochemical analysis of surgically resected GC samples and analyzed the association between *HOXA10* and various markers including the gastric/intestinal phenotypes (*MUC5AC*, *MUC6*, *MUC2* and *CD10*), *CDX2*, β -catenin, *EGFR* and *p53*. Furthermore, we also studied the relationship between *HOXA10* expression and patient prognosis and the effect of *HOXA10* on cell growth, motility and invasion.

Materials and methods

Tissue samples

For microarray analysis, two primary GC samples (W226T: 59-year-old man, T1N0M0, stage I, well-differentiated adenocarcinoma; W246T: 44-year-old man, T2N2M0, stage III, well-differentiated adenocarcinoma) and corresponding non-neoplastic mucosa were used. These GC samples were analyzed previously by SAGE for comprehensive gene expression profiling (5). For quantitative reverse transcription-PCR (RT-PCR) analysis, 38 GC samples and corresponding non-neoplastic mucosa samples were used. The samples were obtained during surgery at the Hiroshima University Hospital. We confirmed microscopically that the tumor specimens were predominantly (>50%) cancer tissue. Samples were frozen immediately in liquid nitrogen and stored at -80°C until use. Samples of normal brain, spinal cord, heart, skeletal muscle, lung, stomach, small intestine, colon, liver, pancreas, kidney, uterus, bone marrow, spleen, peripheral leukocytes and trachea were purchased from Clontech (Palo Alto, CA). For immunohistochemical analysis, we used archival formalin-fixed paraffin-embedded tissues from 749 patients (480 men and 269 women; age range, 29–88 years; mean, 70 years) who had undergone surgical excision for GC at the Hiroshima University Hospital or affiliated hospitals. The 749 GC cases were histologically classified as 429 differentiated type (papillary adenocarcinoma or tubular adenocarcinoma) and 320 undifferentiated type (poorly differentiated adenocarcinoma, signet ring cell carcinoma or mucinous adenocarcinoma), according to the Japanese Classification of Gastric Carcinomas (20). Tumor staging was carried out according to the

International Union Against Cancer TNM classification of malignant tumors. Because written informed consent was not obtained, identifying information for all samples was removed before analysis for strict privacy protection. This procedure was in accordance with the Ethical Guidelines for Human Genome/ Gene Research enacted by the Japanese Government.

Microarray analysis

Gene expression profiles of tissue samples were analyzed by genome-wide microarrays as described previously (21). Affymetrix GeneChip Human Genome U133Plus 2.0 arrays (Affymetrix, Santa Clara, CA) were used. Each transcript on this array is represented by a set of 11 probe pairs, called the probe set. The array contains >54 000 probe sets, representing 47 400 transcripts, including 38 500 genes. Five micrograms of total RNA were used to prepare antisense biotinylated RNA with One-cycle Target Labeling and Control Reagent (Affymetrix) according to the manufacturer's instructions. In brief, first-stranded complementary DNA (cDNA) was synthesized with a T7-RNA polymerase promoter-attached oligo(dT) primer followed by second-stranded cDNA synthesis. This cDNA was purified and served as a template in the subsequent *in vitro* T7-transcription. The *in vitro* T7-transcription reaction was carried out in the presence of T7 RNA polymerase and biotinylated UTP for complementary RNA production. The biotinylated complementary RNAs were then cleaned up and fragmented. The fragmented biotinylated complementary RNA was hybridized to the array (45°C for 16 h). The procedures for staining, washing and scanning of arrays were carried out according to the instructions in the Affymetrix technical manual. The expression value (average difference) of each probe was calculated with GeneChip Operating Software Version 1.1 (Affymetrix). The mean of average difference values in each experiment was 1000 to reliably compare variable multiple arrays.

Quantitative RT-PCR analysis

Total RNA was extracted with an RNeasy Mini Kit (Qiagen, Valencia, CA), and 1 µg of total RNA was converted to cDNA with a First Strand cDNA Synthesis Kit (Amersham Biosciences, Piscataway, NJ). Quantitation of *HOXA10* messenger RNA levels in human tissue samples was done by real-time fluorescence detection as described previously (22). PCR was performed with an SYBR Green PCR Core Reagents Kit (Applied Biosystems, Foster City, CA). The *HOXA10* primer sequences were 5'-AGATATTGTCCTAAGTGTCAGTCCTGA-3' and 5'-GCCAITTCGAGCAGTGGG-3'. Real-time detection of the emission intensity of SYBR Green bound to double-stranded DNA was performed with an ABI PRISM 7700 Sequence Detection System (Applied Biosystems) as described previously (23). *ACTB*-specific PCR products were amplified from the same RNA samples and served as internal controls. We calculated the ratio of *HOXA10* messenger RNA levels between GC tissue (T) and corresponding non-neoplastic mucosa (N). T/N ratios of >2.0 were considered to indicate upregulation.

Antibodies

Goat polyclonal anti-*HOXA10* antibody was purchased from Santa Cruz Biotechnology (Santa Cruz, CA). We used four antibodies for analysis of the GC mucin phenotypes: mouse monoclonal anti-MUC5AC (Novocastra, Newcastle, UK) as a marker of gastric foveolar epithelial cells, mouse monoclonal anti-MUC6 (Novocastra) as a marker of pyloric gland cells, mouse monoclonal anti-MUC2 (Novocastra) as a marker of goblet cells in the small intestine and colorectum and mouse monoclonal anti-CD10 (Novocastra) as a marker of microvilli of absorptive cells in the small intestine and colorectum. In addition, we used mouse monoclonal anti-CDX2 (BioGenex, San Ramon, CA) as a marker of differentiation of intestinal epithelial cells, mouse monoclonal anti-β-catenin (BD Biosciences, San Jose, CA), mouse monoclonal anti-EGFR (Novocastra) and mouse monoclonal anti-p53 (Novocastra).

Western blot analysis

For western blot analysis, tissue samples or cells were lysed as described previously (24). The lysates (40 µg) were solubilized in Laemmli sample buffer by boiling and then subjected to 12% sodium dodecyl sulfate-polyacrylamide gel electrophoresis followed by electrotransfer onto a nitrocellulose filter. Peroxidase-conjugated anti-goat IgG was used in the secondary reaction. Immunocomplexes were visualized with an ECL Western Blot Detection System (Amersham Biosciences). β-actin antibody (Sigma Chemical) was also used as a loading control.

Immunohistochemistry

A Dako LSAB Kit (Dako, Carpinteria, CA) was used for immunohistochemical analysis. In brief, sections were pretreated by microwave treatment in citrate buffer for 15 min to retrieve antigenicity. After peroxidase activity was blocked with 3% H₂O₂ methanol for 10 min, sections were incubated with normal goat serum (Dako) for 20 min to block non-specific antibody binding sites. Sections were incubated with the following primary antibodies: anti-*HOXA10* (diluted 1:50), anti-MUC5AC (1:50), anti-MUC6 (1:50), anti-MUC2 (1:50), anti-CD10

(1:50), anti-CDX2 (1:20), anti-β-catenin (1:50), anti-EGFR (1:50) and anti-p53 (1:50). Sections were incubated with primary antibody for 1 h at 25°C, followed by incubations with biotinylated anti-rabbit/mouse IgG and peroxidase-labeled streptavidin for 10 min each. Staining was completed with a 10 min incubation with the substrate-chromogen solution. The sections were counterstained with 0.1% hematoxylin.

Each molecule was classified according to the percentage of stained cancer cells. Expression was considered to be 'negative' if <10% of cancer cells were stained. When at least 10% of cancer cells were stained, the result of immunostaining was considered 'positive'.

Phenotypic analysis of GC

GC cases were classified into four phenotypes: gastric phenotype, intestinal phenotype, gastric and intestinal mixed phenotype and unclassified phenotype. The criteria (25) for classification of gastric phenotype and intestinal phenotype were as follows. GCs in which >10% of the cells displayed the gastric or intestinal epithelial cell phenotype were gastric phenotype or intestinal phenotype cancers, respectively. Those sections that showed both gastric and intestinal phenotypes were classified as gastric and intestinal mixed phenotype, and those that lacked both the gastric and the intestinal phenotypes were classified as the unclassified phenotype.

GC cell lines

Nine cell lines derived from human GC were used. The TMK-1 cell line was established in our laboratory from a poorly differentiated adenocarcinoma (26). Five GC cell lines of the MKN series (MKN-1, adenocarcinoma cell carcinoma; MKN-7; MKN-28; MKN-74, well-differentiated adenocarcinoma and MKN-45, poorly differentiated adenocarcinoma) were kindly provided by Dr Toshimitsu Suzuki (Fukushima Medical University School of Medicine) (27,28). KATO-III, HSC-39 and HSC-57 cell lines were kindly provided by Dr Morimasa Sekiguchi (University of Tokyo) (29) and Dr Kazuyoshi Yanagihara (Yasuda Women's University) (30), respectively. All cell lines were maintained in RPMI 1640 (Nissui Pharmaceutical Co, Ltd, Tokyo, Japan) containing 10% fetal bovine serum (BioWhittaker, Walkersville, MD) in a humidified atmosphere of 5% CO₂ and 95% air at 37°C.

RNA interference and overexpression of *HOXA10* in cell growth, wound healing assay and *in vitro* invasion assay

To knockdown the endogenous *HOXA10*, RNA interference was performed. Short interfering RNA (siRNA) oligonucleotides for *HOXA10* and a negative control were purchased from Invitrogen (Carlsbad, CA). Three independent oligonucleotides were used for *HOXA10* siRNA as follows: a *HOXA10* siRNA1 sequence, 5'-GAGUUUCUGUCAAUUGUACCUUA-3'; a *HOXA10* siRNA2 sequence, 5'-CCGGGAGCUCACAGCCAACUUUAAU-3' and a *HOXA10* siRNA3 sequence, 5'-CGGCAAAGAGUGGUCGGAAGAAGCG-3'. Transfection was performed using Lipofectamine RNAiMAX (Invitrogen) as described previously (31). Briefly, 60 pmol of siRNA and 10 µl of Lipofectamine RNAiMAX were mixed in 1 ml of RPMI medium (10 nmol/l final siRNA concentration). After 20 min of incubation, the mixture was added to the cells and these were plated on dishes for each assay. Forty-eight hours after transfection, cells were analyzed for all experiments. The cells were seeded at a density of 2000 cells per well in 96-well plates. For constitutive expression of *HOXA10*, cDNA was amplified by PCR and subcloned into pcDNA 3.1 (Invitrogen). Transient transfection was carried out with the FuGENE6 Transfection Reagent (Roche Diagnostics, Indianapolis, IN). Cell growth was monitored after 1, 2 and 4 days by the 3-(4,5-dimethylthiazol-2-yl)-2,5-diphenyl tetrazolium bromide (MTT) assay (32). To evaluate cell motility, a wound healing assay was performed. Cells grown to subconfluence were scraped with a sharp edge to make a cell-free area. Cells migrating into the scraped area were observed and photographs were taken every 12 h after scraping. Modified Boyden chamber assays were performed to examine invasiveness. Cells were plated at 10 000 cells per well in RPMI 1640 medium plus 1% serum in the upper chamber of a transwell insert (8 µm pore diameter; Chemicon, Temecula, CA) coated with Matrigel. Medium containing 10% serum was added in the bottom chamber. After 1 and 2 days, cells in the upper chamber were removed by scraping, and the cells remaining on the lower surface of the insert were stained with CyQuant GR dye to assess the number of cells.

Statistical methods

Correlations between clinicopathological parameters and *HOXA10* staining were analyzed by Fisher's exact test. Kaplan-Meier survival curves were constructed for *HOXA10*, MUC5AC, MUC6, MUC2, CD10 or CDX2-positive and -negative patients to compare survival between both groups. The differences in survival curves between groups were tested for statistical significance by the log-rank test (33). *P* values of <0.05 were considered statistically significant. Univariate and multivariate Cox regression was used to evaluate the associations between clinical covariates and cancer-specific mortality. Hazard ratio and 95% confidence interval were estimated from Cox proportional

hazard models. For all analyses, age was treated as a categorical variable (≤ 65 years of age versus >65 years of age). For final multivariable Cox regression models, all variables were included, which were moderately associated ($P < 0.05$) with cancer-specific mortality.

Results

Identification of upregulated genes in GC through microarray analysis

To identify genes with increased expression in GC, we performed microarray analysis. The gene expression profiles obtained from the two primary GC samples (W226T, W246T) and the corresponding non-neoplastic gastric mucosa samples were compared. The top 20 genes that showed higher expression in the GC samples than in the corresponding non-neoplastic gastric mucosa sample by microarray analysis are each listed in Table I. The gene showing the greatest increase in expression in both GC samples by microarray was *HOXA10*. In our previous report analyzing the *PLUNC* gene, the *HOXA10* gene had the ninth greatest increase in expression in poorly differentiated adenocarcinoma of the stomach (P208T) in the microarray analysis (9). We reported a list of the 20 genes with the greatest increase in expression in these three GC samples compared with normal stomach by SAGE analysis (5). We noted that the 20 most upregulated genes identified by microarray were quite different from those identified by SAGE, indicating that genes upregulated in GC are not always detected with SAGE. We then reviewed the expression level of *HOXA10* with our SAGE data and found that the SAGE tag sequence of *HOXA10*, CATAAAAGGG, did not appear in the W226T, W246T and P208T SAGE data. Because expression of *HOXA10* has not been investigated in GC, we therefore decided to analyze it.

Messenger RNA expression of HOXA10 in systemic normal tissues and GC tissues

Quantitative RT-PCR was performed to investigate the specificity of *HOXA10* expression in 16 normal organs. As shown in Figure 1A, *HOXA10* expression was clearly detected in normal skeletal muscle and to a lesser extent in uterine endometrium, kidney and large intestine. The expression of *HOXA10* was detected at low levels, or

not at all, in other normal organs, including stomach tissue. These results are consistent with those in a previous report (18). Next, we analyzed the expression of *HOXA10* in 38 GC tissue samples and 38 corresponding non-neoplastic mucosa samples by quantitative RT-PCR. Of the 38 GC cases, expression of *HOXA10* was upregulated in 27 (71%) (Figure 1B). Messenger RNA expression levels of *HOXA10* showed no correlations with T grade (depth of tumor invasion), N grade (degree of lymph node metastasis) or the tumor stage.

Immunohistochemical analysis of HOXA10 in GC and its correlation with clinicopathological parameters

To test the specificity of the anti-*HOXA10* antibody, western blotting of lysates from nine GC cell lines was carried out (Figure 2A). The anti-*HOXA10* antibody detected a single band of ~ 41 kD on western blots of MKN-45, MKN-74, TMK-1, HSC-39 and HSC-57 cell extracts. Uterus tissue was used as a positive control of *HOXA10* expression. Using this antibody, we performed immunostaining of *HOXA10* in 749 GC and corresponding non-neoplastic gastric mucosa samples (Figure 1). *HOXA10* expression was detected in 221 of the 749 GCs (30%) and was found in the nucleus of both early GC and advanced GC. Histologically, expression of *HOXA10* was observed more frequently in the differentiated type of GC than in the undifferentiated GC ($P < 0.0001$) (Table II). In non-neoplastic gastric mucosa, *HOXA10* was scarcely expressed in normal gastric mucosa, whereas it was often observed in the nucleus of intestinal metaplasia (Figure 1). Next, we analyzed the relationship between *HOXA10* expression and clinicopathological characteristics. *HOXA10* staining showed a significant inverse correlation with the depth of invasion ($P < 0.0001$). There was no significant association between *HOXA10* staining and other parameters (age, sex, N grade, M grade or stage).

Association of HOXA10 expression with the intestinal mucin phenotype of GC

We investigated the association between *HOXA10* expression and various markers determining the gastric/intestinal mucin phenotypes. Out of the 749 cases examined, each molecule was detected in 437 (58%) cases for MUC5AC, 63 (8%) cases for MUC6, 179 (24%) cases

Table I. The 20 most upregulated genes in both early and advanced GC by microarray analysis

Early GC			Advanced GC				
Symbol	Intensity		Fold	Symbol	Intensity		Fold
	W226T ^a	Non-neoplastic mucosa			W246T ^b	Non-neoplastic mucosa	
<i>LOC339751</i>	6514	7	931	<i>FGFR2</i>	25747	25	1030
<i>SLC19A3</i>	6398	17	376	<i>NOX1</i>	2765	3	922
<i>HOXA13</i>	2619	9	291	<i>IMP-3</i>	5772	11	525
<i>CI4orf105</i>	1104	5	221	<i>HOXA10</i>	6255	16	391
<i>ADH4</i>	41 503	213	195	<i>TMEM16C</i>	1840	5	368
<i>HOXA10</i>	2789	15	186	<i>FLJ21545</i>	3756	13	289
<i>LEFTY1</i>	34 166	249	137	<i>KCNJ3</i>	5488	29	189
<i>ZIC2</i>	400	4	100	<i>CaMKIIα</i>	1928	12	161
<i>SPRR1A</i>	1083	12	90	<i>FLJ38736</i>	3732	29	129
<i>CPS1</i>	92 949	1093	85	<i>NTS</i>	17 320	141	123
<i>CST1</i>	3014	36	84	<i>PPL8</i>	615	5	123
<i>LOC136288</i>	128	2	64	<i>PCLO</i>	1148	10	115
<i>FLJ12971</i>	256	4	64	<i>CHM</i>	111	1	111
<i>FLJ42567</i>	1952	32	61	<i>FLJ42567</i>	3498	33	106
<i>LOC338759</i>	175	3	58	<i>MGC32871</i>	26 808	271	99
<i>LOC196264</i>	172	3	57	<i>CDX1</i>	9581	97	98
<i>NYD-SP20</i>	165	3	55	<i>IMAGE:4806358</i>	22 819	235	97
<i>ADH6</i>	4558	86	53	<i>MGC48998</i>	2287	24	95
<i>CaMKIIα</i>	612	12	51	<i>TFF3</i>	45 055	502	90
<i>CEACAM7</i>	306	6	51	<i>AFP</i>	9018	104	87

^aW226T: 59-year-old man, T1N0M0, stage I, well-differentiated adenocarcinoma.

^bW246T: 44-year-old man, T2N2M0, stage III, well-differentiated adenocarcinoma.

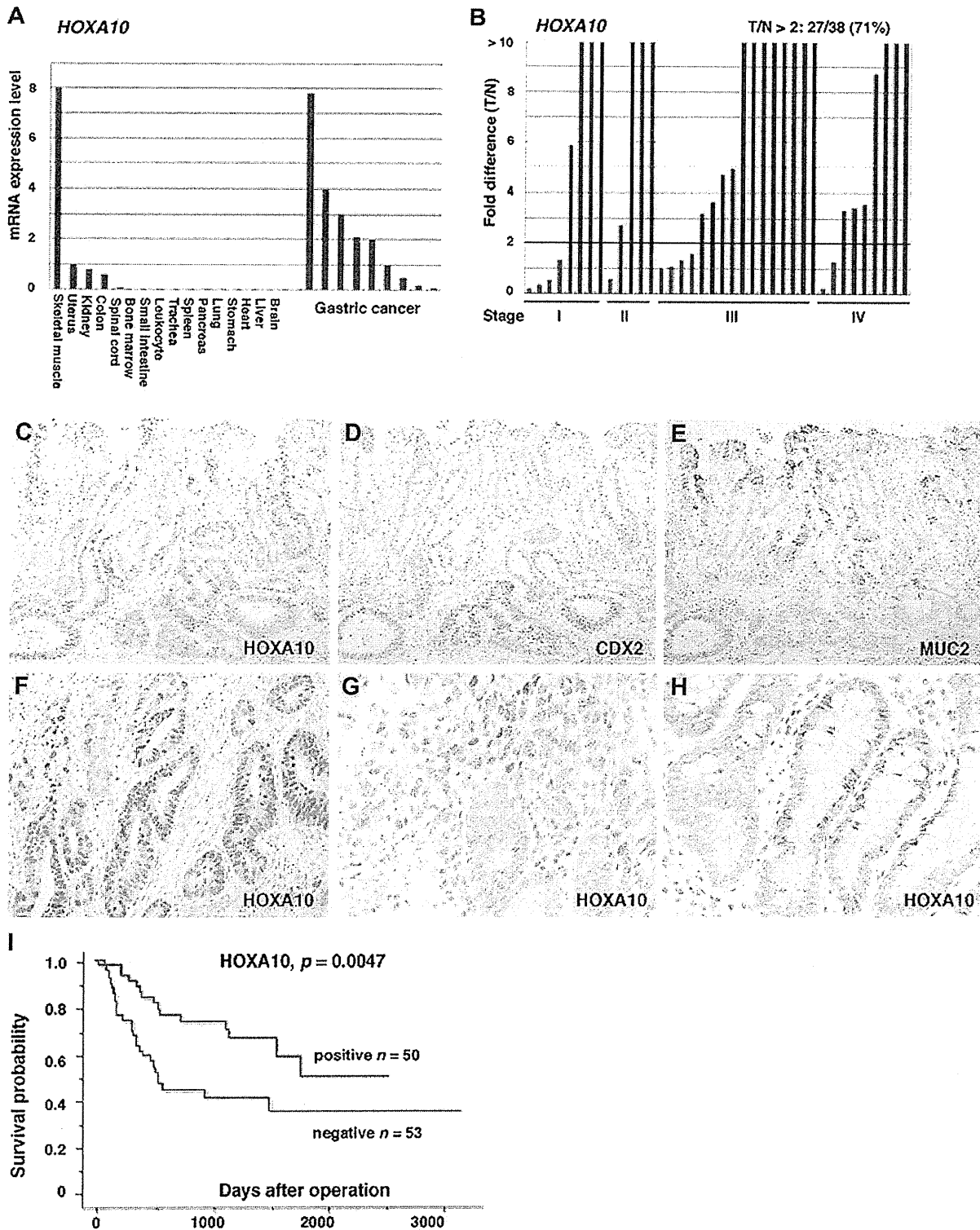


Fig. 1. Quantitative RT-PCR analysis of *HOXA10* in systemic normal tissues, GC tissues and corresponding non-neoplastic mucosa. (A) Clear *HOXA10* expression is present in normal skeletal muscle, uterus, kidney and colon. The units are arbitrary. (B) Fold-change indicates the ratio of *HOXA10* mRNA level in GC (T) to that in the corresponding non-neoplastic mucosa (N). Expression of *HOXA10* was upregulated ($T/N < 2$) in 27 (71%) of 38 GC cases. Immunohistochemical staining of *HOXA10*, *CDX2* and *MUC2* in GC and intestinal metaplasia (C–H), and the relationship between *HOXA10* expression and patient prognosis (I). *HOXA10* was detected in the nucleus of both differentiated (C, F) and undifferentiated GC (G) but not in non-cancerous epithelium, except for intestinal metaplasia (H). The prognosis of patients with positive *HOXA10* expression was significantly better than in the negative cases (I) ($P = 0.0047$, log-rank test). mRNA, messenger RNA.

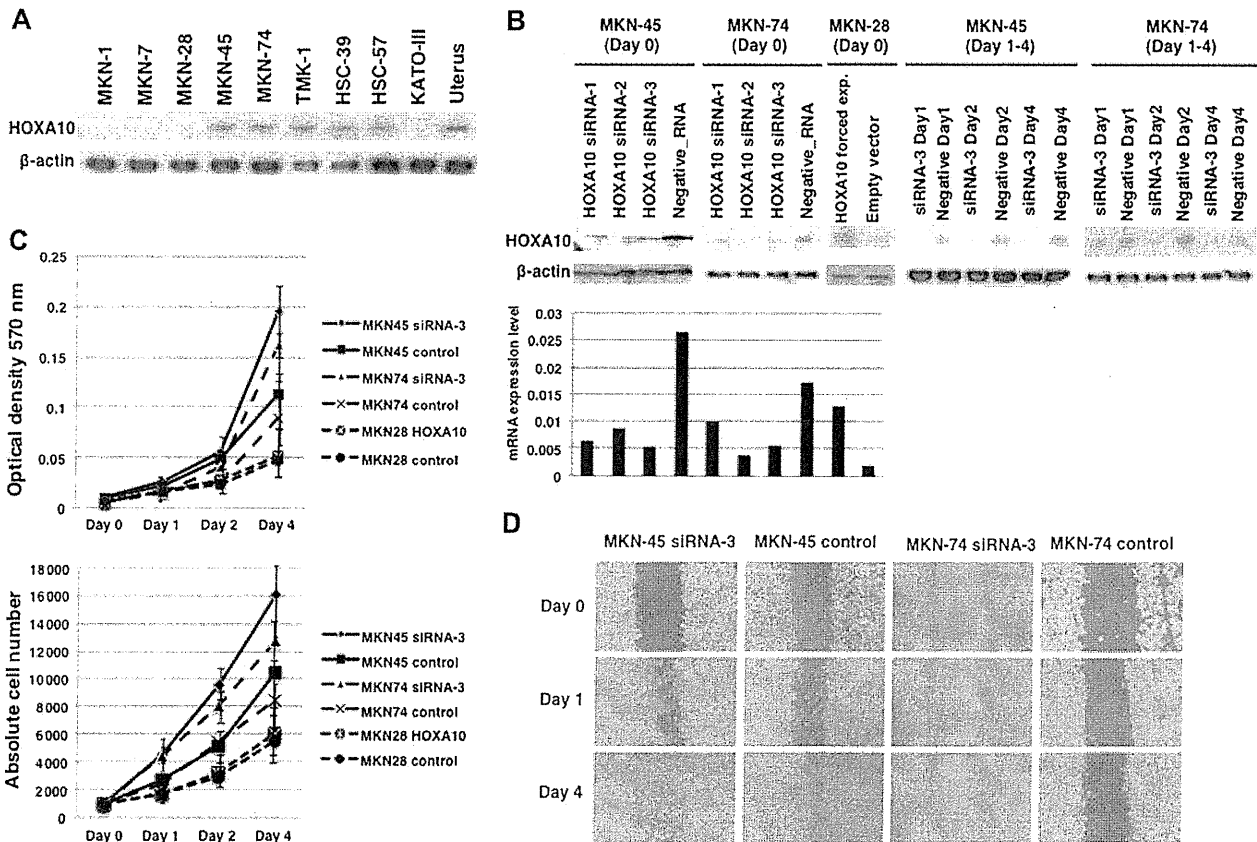


Fig. 2. Effect of *HOXA10* upregulation and downregulation on cell growth and cell motility. The anti-*HOXA10* antibody detected an ~41 kD band on western blots of MKN-45, MKN-74, TMK-1, HSC-39 and HSC-57 cell extracts. Uterus tissue was used as a positive control of *HOXA10* expression (A). Western blotting and quantitative RT-PCR analysis of *HOXA10* expression in MKN-45 and MKN-74 cell lines with *HOXA10* siRNA or control scrambled siRNA transfection (Day 0–4), and MKN-28 cell line transfected with *HOXA10* cDNA or empty vector (Day 0) (B). To investigate the possible involvement of *HOXA10* on cell growth, an 3-(4,5-dimethylthiazole-2-yl)-2,5-diphenyl tetrazolium bromide assay was performed on the fourth day after siRNA or *HOXA10* expression vector transfection (C). Both *HOXA10* siRNA-transfected MKN-45 and MKN-74 cells showed significantly increased viability relative to control scrambled siRNA-transfected cells. Next, effects of *HOXA10* expression on migration potency were determined using a wound healing assay (D). Both *HOXA10* siRNA-transfected MKN-45 and MKN-74 cells migrating into the scratched area were significantly more than negative control cells.

for MUC2 and 70 (9%) cases for CD10. The 749 GC cases were classified into four phenotypes: 297 (40%) were the gastric phenotype, 172 (23%) were the gastric and intestinal mixed phenotype, 130 (17%) were the intestinal phenotype and 150 (20%) were the unclassified phenotype. Positive expression of *HOXA10* was significantly more frequent in MUC2-positive cases than MUC2-negative cases ($P < 0.0001$) (Figure 1 and Table III). *HOXA10* expression occurred more frequently in the intestinal phenotype and the gastric and intestinal mixed phenotype than in the gastric phenotype and the unclassified phenotype ($P = 0.0004$). On the other hand, CDX2 was detected in 195 of the 749 (26%) cases, and positive expression of *HOXA10* was significantly more frequent in CDX2-positive cases than CDX2-negative cases ($P = 0.0003$) (Figure 1 and Table III). The other molecules were detected in 245 (33%) cases for β -catenin, 99 (13%) cases for EGFR and 257 (34%) cases for p53. There was no clear relationship between expression of *HOXA10* and these markers.

Relationship between expression of *HOXA10* in GC and patient prognosis

We also examined the relationship between survival and expression of *HOXA10*, CDX2 and mucins (MUC5AC, MUC6, MUC2 and CD10) in 103 GCs. The prognosis of patients with positive *HOXA10* expression was significantly better than in the negative cases (Figure 11) ($P = 0.0047$, log-rank test). The expression of the other molecules had

no significant effect on the prognosis of patients (CDX2, $P = 0.1426$; MUC5AC, $P = 0.3936$; MUC6, $P = 0.9835$; MUC2, $P = 0.4996$; CD10, $P = 0.27$). In order to evaluate the potential for *HOXA10* expression as a prognostic classifier, both univariate and multivariate Cox proportional hazards analyses were used to further evaluate the association of *HOXA10* expression with cancer-specific mortality (Table IV). In univariate analysis, negative expression of *HOXA10* (hazard ratio, 0.41; 95% confidence interval, 0.22–0.78; $P = 0.006$) and the TNM stage (hazard ratio, 6.13; 95% confidence interval, 2.84–13.3; $P < 0.0001$) was associated with survival. In the multivariate model, negative expression of *HOXA10* expression and TNM stage was independent predictors of survival in patients with GC (Table IV).

Effect of *HOXA10* upregulation and downregulation on cell growth, cell motility and invasive activity

HOXA10 staining showed a significant inverse correlation with the depth of invasion, suggesting that *HOXA10* may be associated with tumor progression. However, the biological significance of *HOXA10* in GC has not been studied. To investigate the possible involvement of *HOXA10* on cell growth, an MTT assay was performed on the fourth day after *HOXA10* siRNA or control scrambled siRNA transfection in the MKN-45 and MKN-74 cell lines and MKN-28 cell line transfected with *HOXA10* expression vector (pcDNA-*HOXA10*) or empty vector.

Table II. Relation between HOXA10 expression and clinicopathological parameters in 749 cases of GC

Factor	HOXA10 expression		P value
	Positive (n = 221)	Negative (n = 528)	
Age			
≤65 years (n = 359)	95 (26%)	264	NS
>65 years (n = 390)	126 (32%)	264	
Sex			
Male (n = 480)	137 (29%)	343	NS
Female (n = 269)	84 (31%)	185	
T grade ^a			
T1/T2 (n = 608)	216 (36%)	392	<0.0001
T3/T4 (n = 141)	5 (4%)	136	
N grade ^a			
N0 (n = 433)	131 (30%)	302	NS
N1/N2/N3 (n = 316)	90 (28%)	226	
M grade ^a			
M0 (n = 742)	217 (29%)	525	NS
M1 (n = 7)	4 (57%)	3	
Stage ^a			
Stage 0/I (n = 425)	130 (31%)	295	NS
Stage II/III/IV (n = 324)	91 (28%)	233	
Histology ^b			
Differentiated (n = 429)	152 (35%)	277	<0.0001
Undifferentiated (n = 320)	69 (22%)	251	

P values were calculated by Fisher's exact test. NS, not significant.

^aTumor stage was classified according to the criteria of the International Union Against Cancer TNM classification of malignant tumors.

^bHistology was determined according to the Japanese Classification of Gastric Cancer.

Table III. Relation between HOXA10 expression and various molecules including mucin-related markers in 749 cases of GC

Molecule	HOXA10 expression		P value
	Positive (221)	Negative (528)	
MUC5AC			
Positive	140 (32%)	297	NS
Negative	81 (26%)	231	
MUC6			
Positive	22 (35%)	41	NS
Negative	199 (29%)	487	
MUC2			
Positive	79 (44%)	100	<0.0001
Negative	142 (25%)	428	
CD10			
Positive	17 (24%)	53	NS
Negative	204 (30%)	485	
CDX2			
Positive	78 (40%)	117	0.0003
Negative	143 (26%)	411	
β-catenin			
Positive	69 (28%)	176	NS
Negative	152 (30%)	352	
EGFR			
Positive	32 (32%)	67	NS
Negative	189 (29%)	461	
p53			
Positive	79 (31%)	178	NS
Negative	142 (29%)	350	

P values were calculated by Fisher's exact test. EGFR, epidermal growth factor receptor; NS, not significant.

At first, we checked the upregulation or downregulation of HOXA10 from day 0 to day 4, using western blotting or quantitative RT-PCR analysis (Figure 2B). Both HOXA10 siRNA-transfected MKN-45 and

Table IV. Univariate and multivariate Cox regression analysis of HOXA10 expression and overall survival in 134 cases of GC

Factor	Univariate analysis		Multivariate analysis	
	HR (95% CI)	P value	HR (95% CI)	P value
Age				
≤65 years	1 (Reference)	0.15		
>65 years	1.82 (0.81–4.12)			
Sex				
Female	1 (Reference)	0.29		
Male	1.39 (0.75–2.58)			
HOXA10				
Negative	1 (Reference)	0.006	1 (Reference)	0.0044
Positive	0.41 (0.22–0.78)		0.39 (0.21–0.75)	
CDX2				
Negative	1 (Reference)	0.15		
Positive	0.58 (0.28–1.21)			
MUC5AC				
Negative	1 (Reference)	0.39		
Positive	0.76 (0.41–1.42)			
MUC6				
Negative	1 (Reference)	0.98		
Positive	1.01 (0.36–2.83)			
MUC2				
Negative	1 (Reference)	0.51		
Positive	0.77 (0.35–1.66)			
CD10				
Negative	1 (Reference)	0.27		
Positive	1.54 (0.71–3.32)			
TNM stage ^a				
Stage 0/I	1 (Reference)	<0.0001	1 (Reference)	0.0044
Stage II/III/IV	6.13 (2.84–13.3)		6.45 (2.94–14.1)	
Histology ^b				
Differentiated	1 (Reference)	0.29		
Undifferentiated	1.41 (0.75–2.63)			

CI, confidence interval; HR, hazard ratio.

^aTNM stage was classified according to the criteria of the International Union Against Cancer TNM classification of malignant tumors.

^bHistological type was determined according to the Japanese Classification of Gastric Cancer.

MKN-74 cells showed significantly increased viability relative to negative control cells, whereas cell viability of pcDNA-HOXA10 was not different from those of a negative control vector (Figure 2C). Next, effects of HOXA10 expression on migration potency were determined using a wound healing assay. Both HOXA10 siRNA-transfected MKN-45 and MKN-74 cells migrating into the scratched area were significantly more than negative control cells (Figure 2D), whereas cell motility of pcDNA-HOXA10 was not different from those of a negative control vector (data not shown). In addition, a transwell invasion assay was performed in the MKN-45 and MKN-74 cell lines to determine the possible role of HOXA10 in the invasiveness of GC cells. Invasion ability was not significantly different between HOXA10 knockdown GC cells and control GC cells (data not shown). These results indicate that HOXA10 inhibits cell growth and cell motility but not invasion in GC cells.

Discussion

In the present study, we studied the gene expression profile using microarray data of GC samples that were previously analyzed by SAGE (5) and identified that the *HOXA10* gene was upregulated in all samples. Quantitative RT-PCR in 38 GC samples revealed that *HOXA10* was overexpressed in >70% of GCs. Because upregulation of HOXA10 was identified by microarray and quantitative RT-PCR analysis of bulk GC tissues, immunohistochemistry was required to determine whether cancer cells truly express HOXA10. Immunohistochemical analysis revealed that HOXA10-positive cancer cells were detected in 221 (30%) of the 749 GC cases. HOXA10 was frequently

expressed in MUC2-positive GC cases, and HOXA10 expression was observed at high levels in GC with intestinal mucin phenotype. Ectopic CDX2 expression plays an important role in the development of GC with intestinal phenotype (34,35). Here, we also showed that HOXA10 expression was correlated with CDX2 expression in GC tissue. A previous report indicated that overexpression of CDX2 with the N-terminal transactivation domain upregulated HOXA10 gene expression in murine bone marrow progenitors (19). Taken together, expression of HOXA10, in addition to CDX2, may be a key factor mediating the development of GC with the intestinal mucin phenotype.

In non-neoplastic gastric mucosa, HOXA10 was scarcely expressed in normal gastric mucosa. However, we often observed nuclear accumulation of HOXA10 in intestinal metaplasia. The findings that HOXA10 expression is observed in intestinal metaplasia as well as in GC with the intestinal phenotype imply that this change occurs at an early stage of stomach carcinogenesis. Aberrations of DNA methylation are now believed to be an important epigenetic alteration occurring early in many cancers (36). In addition, it has been reported that there is a relationship between aberrant methylation of *HOXA10* and its protein expression in ovarian cancer and endometrial cancer (18,37). We speculated that aberrant promoter hypomethylation of the *HOXA10* gene leads to high expression of HOXA10 in GC.

In immunohistochemical analysis, there was a significant inverse correlation between HOXA10 expression and tumor progression. In addition, the prognosis of patients with positive HOXA10 expression was significantly better than that of negative cases. The previous reports showed that enforced expression of HOXA10 in endometrial carcinoma cells inhibited invasive behavior through downregulating Snail expression and inducing E-cadherin expression (18) and that increased HOXA10 in breast cancer cells regulated p53 expression toward reduction of invasiveness (38). HOXA10 was reported to bind to the *p21* promoter and activate *p21* transcription, resulting in cell cycle arrest and differentiation in differentiating myelomonocytic cells (15). Furthermore, Sugimoto *et al.* (39) reported that the expression of HOXA10 has an important role in apoptosis induction of chronic myelogenous leukemia cells treated with tyrosine kinase inhibitors. In the present study, knockdown of HOXA10 by siRNA had an effect on cell growth and cell motility in the GC cell line but not on cell invasion. Furthermore, we observed a higher expression of HOXA10 in the differentiated type of GC compared with the undifferentiated type. This may reflect a loss of ability to express this protein along with a decrease in histological differentiation in neoplastic cells. Once malignant formation is completed, HOXA10 might deregulate the progression of GC. It is possible that loss of *HOXA10* expression could lead to tumor progression by promoting epithelial–mesenchymal transition (18). There was no clear relationship between expression of HOXA10 and β -catenin, EGFR and p53. Further studies should be performed in the near future to elucidate the tissue specificity of the detailed pathways involving HOXA10.

In the present study, we compared gene expression profiles of GC samples analyzed by microarray analysis and SAGE. The 20 genes showing the greatest increase in expression on the microarrays were quite different from those obtained with the SAGE library. Investigation of the difference between microarray analysis and SAGE is beyond the scope of the present study and will be described elsewhere.

In summary, we demonstrated that HOXA10 is frequently upregulated in GC with the intestinal mucin phenotype and HOXA10 expression correlates with favorable survival in patients with GC. HOXA10 expression may be a key factor mediating the biological behavior of the intestinal phenotype of GC.

Funding

This work was supported, in part, by grants-in-aid for Cancer Research from the Ministry of Education, Culture, Sports and Technology of Japan and in part by a grant-in-aid for the Third Comprehensive 10-year Strategy for Cancer Control and for Cancer Research from the Ministry of Health, Labour and Welfare of Japan.

Acknowledgements

We thank Mr Shinichi Norimura for his excellent technical assistance and advice. This work was carried out with the kind cooperation of the Research Center for Molecular Medicine, Faculty of Medicine, Hiroshima University. We also thank the Analysis Center of Life Science, Hiroshima University, for the use of their facilities.

Conflict of Interest Statement: None declared.

References

- Yasui, W. *et al.* (2005) Recent advances in molecular pathobiology of gastric carcinoma. In Kaminishi, M., Takubo, K. and Mafune, K. (eds) *The Diversity of Gastric Carcinoma: Pathogenesis, Diagnosis and Therapy*. Springer, Tokyo, Japan, 51–71.
- Yasui, W. *et al.* (2004) Search for new biomarkers of gastric cancer through serial analysis of gene expression and its clinical implications. *Cancer Sci.*, **95**, 385–392.
- Lockhart, D.J. *et al.* (1996) Expression monitoring by hybridization to high-density oligonucleotide arrays. *Nat. Biotechnol.*, **14**, 1675–1680.
- Velculescu, V.E. *et al.* (1995) Serial analysis of gene expression. *Science*, **270**, 484–487.
- Oue, N. *et al.* (2004) Gene expression profile of gastric carcinoma: identification of genes and tags potentially involved in invasion, metastasis, and carcinogenesis by serial analysis of gene expression. *Cancer Res.*, **64**, 2397–2405.
- Ferguson, D.A. *et al.* (2005) Selective identification of secreted and transmembrane breast cancer markers using *Escherichia coli* ampicillin secretion trap. *Cancer Res.*, **65**, 8209–8217.
- Oue, N. *et al.* (2005) Expression and localization of Reg IV in human neoplastic and non-neoplastic tissues: Reg IV expression is associated with intestinal and neuroendocrine differentiation in gastric adenocarcinoma. *J. Pathol.*, **207**, 185–198.
- Sentani, K. *et al.* (2008) Immunohistochemical staining of Reg IV and claudin-18 is useful in the diagnosis of gastrointestinal signet ring cell carcinoma. *Am. J. Surg. Pathol.*, **32**, 1182–1189.
- Sentani, K. *et al.* (2008) Gene expression profiling with microarray and SAGE identifies PLUNC as a marker for hepatoid adenocarcinoma of the stomach. *Mod. Pathol.*, **21**, 464–475.
- Sentani, K. *et al.* (2010) Upregulation of connexin 30 in intestinal phenotype gastric cancer and its reduction during tumor progression. *Pathobiology*, **77**, 241–248.
- Anami, K. *et al.* (2010) Search for transmembrane protein in gastric cancer by the *Escherichia coli* ampicillin secretion trap: expression of DSC2 in gastric cancer with intestinal phenotype. *J. Pathol.*, **221**, 275–284.
- McGinnis, W. *et al.* (1992) Homeobox genes and axial patterning. *Cell*, **68**, 283–302.
- Chen, K.N. *et al.* (2005) Expression of 11 HOX genes is deregulated in esophageal squamous cell carcinoma. *Clin. Cancer Res.*, **11**, 1044–1049.
- Lawrence, H.J. *et al.* (1992) Homeobox genes in normal hematopoiesis and leukemia. *Blood*, **80**, 2445–2453.
- Bromleigh, V.C. *et al.* (2000) p21 is a transcriptional target of HOXA10 in differentiating myelomonocytic cells. *Genes Dev.*, **14**, 2581–2586.
- Slany, R.K. (2005) When epigenetics kills: MLL fusion proteins in leukemia. *Hematol. Oncol.*, **23**, 1–9.
- Sarno, J.L. *et al.* (2005) HOXA10, Pbx2, and Meis1 protein expression in the human endometrium: formation of multimeric complexes on HOXA10 target genes. *J. Clin. Endocrinol. Metab.*, **90**, 522–528.
- Yoshida, H. *et al.* (2006) Deregulation of the HOXA10 homeobox gene in endometrial carcinoma: role in epithelial–mesenchymal transition. *Cancer Res.*, **66**, 889–897.
- Rawat, V.P. *et al.* (2008) Overexpression of CDX2 perturbs HOX gene expression in murine progenitors depending on its N-terminal domain and is closely correlated with deregulated HOX gene expression in human acute myeloid leukemia. *Blood*, **111**, 309–319.
- Japanese Gastric Cancer Association. (2011) Japanese classification of gastric carcinoma: 3rd English edition. *Gastric Cancer*, **14**, 101–112.
- Nishigaki, M. *et al.* (2005) Discovery of aberrant expression of R-RAS by cancer-linked DNA hypomethylation in gastric cancer using microarrays. *Cancer Res.*, **65**, 2115–2124.
- Gibson, U.E. *et al.* (1996) A novel method for real time quantitative RT-PCR. *Genome Res.*, **6**, 995–1001.
- Kondo, T. *et al.* (2004) Expression of POT1 is associated with tumor stage and telomere length in gastric carcinoma. *Cancer Res.*, **64**, 523–529.

24. Yasui, W. *et al.* (1993) Increased expression of p34cdc2 and its kinase activity in human gastric and colonic carcinomas. *Int. J. Cancer*, **53**, 36–41.
25. Mizoshita, T. *et al.* (2003) Expression of Cdx2 and the phenotype of advanced gastric cancers: relationship with prognosis. *J. Cancer Res. Clin. Oncol.*, **129**, 727–734.
26. Ochiai, A. *et al.* (1985) Growth-promoting effect of gastrin on human gastric carcinoma cell line TMK-1. *Jpn. J. Cancer Res.*, **76**, 1064–1071.
27. Hojo, H. *et al.* (1977) Establishment of cultured cell lines of human stomach cancer origin and their morphological characteristics. *Niigata Igakkai Zasshi*, **91**, 737–763.
28. Motoyama, T. *et al.* (1986) Comparison of seven cell lines derived from human gastric carcinomas. *Acta Pathol. Jpn.*, **36**, 65–83.
29. Sekiguchi, M. *et al.* (1978) Establishment of cultured cell lines derived from a human gastric carcinoma. *Jpn. J. Exp. Med.*, **48**, 61–68.
30. Yanagihara, K. *et al.* (1991) Establishment and characterization of human signet ring cell gastric carcinoma cell lines with amplification of the c-myc oncogene. *Cancer Res.*, **51**, 381–386.
31. Sakamoto, N. *et al.* (2010) Serial analysis of gene expression of esophageal squamous cell carcinoma: ADAMTS16 is upregulated in esophageal squamous cell carcinoma. *Cancer Sci.*, **101**, 1038–1044.
32. Alley, M.C. *et al.* (1988) Feasibility of drug screening with panels of human tumor cell lines using a microculture tetrazolium assay. *Cancer Res.*, **48**, 589–601.
33. Mantel, N. (1966) Evaluation of survival data and two new rank order statistics arising in its consideration. *Cancer Chemother. Rep.*, **50**, 163–170.
34. Tatematsu, M. *et al.* (2003) Stem cells and gastric cancer: role of gastric and intestinal mixed intestinal metaplasia. *Cancer Sci.*, **94**, 135–141.
35. Silberg, D.G. *et al.* (2002) Cdx2 ectopic expression induces gastric intestinal metaplasia in transgenic mice. *Gastroenterology*, **122**, 689–696.
36. Feinberg, A.P. *et al.* (2004) The history of cancer epigenetics. *Nat. Rev. Cancer*, **4**, 143–153.
37. Cheng, W. *et al.* (2010) Identification of aberrant promoter hypomethylation of HOXA10 in ovarian cancer. *J. Cancer Res. Clin. Oncol.*, **136**, 1221–1227.
38. Chu, M.C. *et al.* (2004) HOXA10 regulates p53 expression and matrigel invasion in human breast cancer cells. *Cancer Biol. Ther.*, **3**, 568–572.
39. Sugimoto, Y. *et al.* (2008) HOXA10 expression induced by Abl kinase inhibitors enhanced apoptosis through PI3K pathway in CML cells. *Leuk. Res.*, **32**, 962–971.

Received November 3, 2011; revised February 19, 2012;
accepted March 3, 2012